USE OF RADARSAT-2 POLARIMETRIC SAR IMAGES FOR DROUGHT CODE MAPPING OVER CANADIAN PRAIRIE GRASSLANDS

by

Duncan Dawson Rand, P.Eng.

Postgraduate Diploma in Geographical Information Systems with Distinction, University of Salford, 2012

Bachelor of Science in Civil Engineering, University of Alberta, 1992

A Thesis Submitted in Partial Fulfillment
of the Requirements for the Degree of

Master of Science in Forest Engineering

in the Graduate Academic Unit of Faculty of Forestry & Environmental Management

Supervisors: Brigitte Leblon, PhD, Forestry & Environmental Management, Co-Supervisor
Joseph Buckley, PhD, Royal Military College/Honorary Research Associate-Forestry & Environmental Management, Co-Supervisor
Laura Bourgeau-Chavez, PhD, Michigan Tech Research Institute

Examining Board: Marek Krasowski, PhD, Forestry & Environmental Management, Chair
Renaud Mathieu, PhD, Council for Scientific and Industrial Research/Honorary Research Associate-Forestry & Environmental Management
William Ward, PhD, Physics

This thesis is accepted by the
Dean of Graduate Studies

THE UNIVERSITY OF NEW BRUNSWICK

May, 2016

ABSTRACT

To enable fire danger mapping, the Canadian Fire Weather Index System's drought code (DC) component needs to be determined. This study reports test results on the use of C-Band polarimetric synthetic aperture radar images to assess DC levels over Canadian Prairies grasslands. Forty-five RADARSAT-2 images acquired for the 2008-2012 fire seasons were analyzed to determine those corresponding to the extreme wet, extreme dry, and in-season wet DC conditions. These were used to compute a number of polarimetric parameters which were compared to identify which vary most significantly over the DC conditions within eight vegetation classes in the study area. The results show statistically significant differences for a number of parameters demonstrating their utility to distinguish between DC conditions independent of seasonal vegetation changes. The current study will enable further research to develop algorithms predicting DC values which would permit remote estimation of fire danger conditions on the Canadian Prairies grasslands.

ACKNOWLEDGEMENTS

RADARSAT-2 imagery was provided by the Canadian Space Agency through the Department of National Defence. Thanks to Maria West for her patience and encouragement.

Table of Contents

List of Tables

List of Figures

Introduction

Fire is an important and integral component of Canada's natural landscape; whether its origin is natural lightning or human ignition, or that landscape is forest or grassland, alpine or plains, fire both destroys and renews the natural landscape at the same time. The Canadian Prairies are no exception to this concurrent destructive and constructive force, and indeed owe their existence and expansion to the results of fire (Axelrod, 1985; Rannie, 2001; Bailey et al., 2010). Within the Canadian Prairies, there are five eco-regions consisting of dry mixed grass prairie, mixed grass prairie, foothills fescue, parkland-northern fescue, and tall grass prairie (Bailey et al., 2010). Natural fires in these ecosystems burn vegetation, including invasive species, and allow the renewal of healthy grasslands to such an extent that historically fire was the "*primary barrier to the reestablishment of forests and woodlands*" (Axelrod, 1985, p.192). However, fire in these ecoregions can also be detrimental by degrading air quality, affecting wildlife and habitat, and if unchecked, causing economic distress through the destruction of property and livestock.

In Canada, fire danger is rated daily using the Canadian Forest Fire Danger Rating System (CFFDRS), a semi-empirical modular system that uses weather, fuel, topography and ignition parameters as inputs through four subsystems (Stocks et al., 1989). One of the subsystems, the Canadian Fire Weather Index (FWI) system, computes potential mid-afternoon fire danger from noon-time weather station records of dry bulb temperature, relative humidity, 10 m high open wind speed, and 24-hour precipitation measurements

(Van Wagner, 1987). The FWI system is comprised of three moisture codes: the Fine Fuel Moisture Code (FFMC) represents quick-drying surface litter fine fuel moisture contents, the Duff Moisture Code (DMC) represents slow-drying moderate depth loosely compact duff moisture contents, and the Drought Code (DC) represents slow-drying deep layer compact organic matter moisture contents. These three moisture codes have time lags of two-thirds of a day, 15 days, and 53 days, respectively (Lawson & Armitage, 2008). Time lags represent the time necessary for a fuel type to lose about two-thirds of its free moisture at equilibrium (when air temperature is 20°C and relative humidity is 40%) (Van Wagner, 1987). Derived from these three moisture codes and wind speed, two indices provide a measure of the initial fire spread rate, the Initial Spread Index (ISI), and the total fuel available for combustion, the Build-up Index (BUI). The FWI is then calculated from the combination of ISI and BUI (Van Wagner, 1987).

The FWI is a useful measure of general fire danger for administrative purposes over large geographic regions (Stocks et al., 1989). However, the FWI system does not consider environmental conditions at finer spatial scales, since it uses point measurements from often widely dispersed weather stations. Fuel moisture measurements made at weather stations, from meteorological variables, are limited spatially because accuracy decreases as the distance between weather station increases. Satellite remote sensing can potentially complement the current fire danger measurements because it can map several CFFDRS parameters. These parameters are not only related to topography, plant phenology and fuel type, but also to fuel moisture, which is an important FWI system parameter. In previous studies, fuel moisture has been estimated primarily from NOAA-AVHRR

normalized difference vegetation index (NDVI) images alone, or in combination with thermal infrared images over forested areas (see reviews by Leblon, 2001; 2005; Leblon et al., 2014) and grasslands (Merzouki & Leblon, 2011). An unavoidable problem of using optical and thermal-infrared remotely sensed images is pixel contamination caused by clouds and atmospheric interferences. Active microwave radar does not suffer these drawbacks, as it is able to penetrate clouds.

Single-polarized SAR images, such as the RADARSAT-1 C-HH and ERS-1 C-VV SAR images, have been used to produce empirical models to predict soil moisture over bare agricultural soils (see the review by Baghdadi et al., 2007) and over natural grasslands (Wagner et al., 1999; 2000; Oldak et al., 2003; Thoma et al., 2006). They also have been used to estimate DC values over boreal forests (Leblon et al., 2002; Abbott et al., 2007; Bourgeau-Chavez et al., 1999;; 2007; 2008). Over vegetated areas, retrieval of soil moisture is more challenging because of the vegetation effects as multiple scattering interactions begin to dominate over the surficial Bragg scattering alone. The resulting backscattered radar energy is thereby influenced by both the physical structure and moisture of vegetation and soil as well as by the interactions between them. Indeed, it is not just that volume scattering becomes dominant, but that the vegetation can hide the surface altogether from the radar as the microwave signal cannot penetrate very far into vegetation. This lack of penetration depth is more severe in the shorter wavelength radars such as X-band (2.4-3.8cm) and C-band (3.8-7.5cm) than in longer such as L-band (15.0-30.0cm). Further complicating the vegetation penetration issue is incidence angle, in general, the larger the incidence angle (i.e. further from the nadir) the lower the

penetration depth as the microwave signal must pass through a greater amount of vegetation than it would closer to nadir (Ulaby *et al.*, 1982).

Methods have been developed to account for these confusing factors and improve the accuracy of soil moisture or DC predictions which include grouping areas by vegetation type (Bourgeau-Chavez et al., 1999; Leblon et al., 2002; Oldak et al., 2003; Abbott et al., 2007), and the use of time-series data (Wagner et al., 1999; 2000; Bourgeau-Chavez, Garwood, et al., 2007; Kim & van Zyl, 2009; van Zyl & Kim, 2011).

The next generation SAR satellites, such as RADARSAT-2 and TerraSAR-X are polarimetric capable of transmitting and receiving on all four possible combinations of horizontal and vertical polarization. The major advantage of using polarimetric SAR over single-polarized SAR is its ability to measure all the polarization characteristics of an area simultaneously. Polarimetric data provides the opportunity to develop soil moisture retrieval algorithms without the need for additional information regarding the surface roughness and vegetation structure, through the use of polarimetric discriminators (van Zyl et al., 1987; Touzi et al., 1992), and polarimetric decompositions (Cloude & Pottier, 1997; Freeman & Durden, 1998; Touzi, 2007; van Zyl et al., 2011). Decomposition techniques help determine the fundamental scattering mechanisms involved in the backscattering of the imaged area. For soil moisture determination they allow either a direct separation of the effect of soil moisture and roughness on the backscatter, or a parameterization of both effects within the scattering.

Polarimetric SAR data have been used to estimate soil moisture over vegetated agricultural fields (Stiles et al., 2000; Hajnsek et al., 2009; Trudel et al., 2012), natural alpine grasslands (Pasolli et al., 2011), and boreal forests (Bourgeau-Chavez et al., 2013a, 2013b), Over alpine meadows and pastures, Pasolli et al. (2011) showed that the use of HH and HV returns improved soil moisture determination, as HV was effective removing the vegetation effect. However Cloude-Pottier decomposition parameters were less effective possibly owing to anisotropy's dependence on local incidence angle accentuated in the alpine environment (Pasolli et al., 2011). Working in the boreal forest ecosystem, Bourgeau-Chavez *et al.* (2013a; 2013b) also noted the lack of sensitivity to site moisture of the Cloude-Pottier decomposition parameters, and attributed this to the sensitivity of the Cloude-Pottier decomposition parameters to biomass and surface roughness, and the lack of account for backscattering intensity information. This is consistent with the nature of the Cloude-Pottier decomposition which seeks to determine the "dominant "average" scattering mechanism in each cell" (Cloude & Pottier, 1997, p.68) based on its physical structure and we would not expect changes in soil moisture (or DC) to affect this response. They did, however, find that C-HH and C-LR polarized backscatter, and the surface power from both Freeman-Durden and van Zyl decompositions showed distinct differences between wet and dry conditions. They also found that the maximum degree of polarization improved the performance of moisture retrieval algorithm, as it "*appears to provide information on the structural complexity of the landscape (surface roughness and/or high biomass) to aid in extraction of surface soil moisture from the SAR data*" (Bourgeau-Chavez, *et al.*, 2013a, p.84). Kong *et al.* (2014) used Bourgeau-Chavez *et al's*(2013a) method, to compare RADARSAT-2 polarimetric SAR imagery that were

acquired under an extreme dry and an extreme wet date (as indicated by the DC value) over *herbaceous* and *shrub and tree* sites in the South African *Lowveld* savannah. Their results show C-HH, C-HV, C-RR, and C-LL, as well as Freeman-Durden and van Zyl decompositions, and the maximum and minimum of several polarimetric discriminators, such as received power, and the scattered intensity all have significant differences between the extreme wet and dry conditions in this ecosystem.

The current study uses the methods presented by Bourgeau-Chavez *et al.* (2013a) in a boreal forest ecosystem, and used by Kong (2014) in South African *Lowveld* savannah to examine the potential of using RADARSAT-2 polarimetric SAR images for detecting extreme drought and wetness over natural mixed-grass prairies in southern Manitoba, Canada. Daily DC values have been determined from available weather records for the study area and extreme wet and dry images have been selected from a time-series of images. In addition to the extreme wet and dry images, an additional image was selected which represents the wettest condition in the same vegetation growing season as the extreme dry image; this image is referred to as the "in-season" wet condition. This in-season wet and dry comparison was not conducted in the above noted studies (Bourgeau-Chavez et al. 2013a, Kong et al. 2014) and is intended to account for the seasonal difference in vegetation states that occur between the extreme wet and dry date comparison noted in those studies. The images were used to compute polarimetric variables for eight regions of interest based on the vegetation cover classes defined in previous work by Buckley (2002; 2004; 2008). All the images were acquired using the

same beam mode (FQ18) and descending orbit, so both factors should not influence the comparison.

Study Area

The study area is Canadian Forces Base (CFB) Shilo which is located in southern Manitoba 35km east of Brandon (Figure 1) and centered at Lat/Long N49° 45' 00" W099° 30' 00". CFB Shilo is a Canadian military training base approximately 40 000 ha in size, and as it has been used for this purpose since 1932. It "is environmentally important since it contains the last remnants of native prairie ecosystems in a region of intense agricultural activity" (Buckley, 2004, p.510), with mixed-grass and parkland-northern fescue being the dominant ecoregions. The majority of the CFB Shilo training area lies on well- to rapidly-drained, sandy aeolian, and sand and gravel soils with topographical slopes of generally less than 5° on the western half of the area increasing to between 15 and 30° on the eastern half. The Assiniboine River borders the study area on the south with the Épinette Creek and associated marshland running through the area from the northeast to centre of the eastern boundary; overland drainage is generally toward these two catchments. This relatively flat landscape will reduce the surface roughness effect due to topography on the radar backscatter and should improve the extraction of soil moisture data. While this base represents native prairie, it may not in all locations be in pristine condition as the intensity of military training can disrupt the topography and "create bare patches within the mixed grass prairie", and alter "the frequency of fires" (Rowland, 2003, p.5).

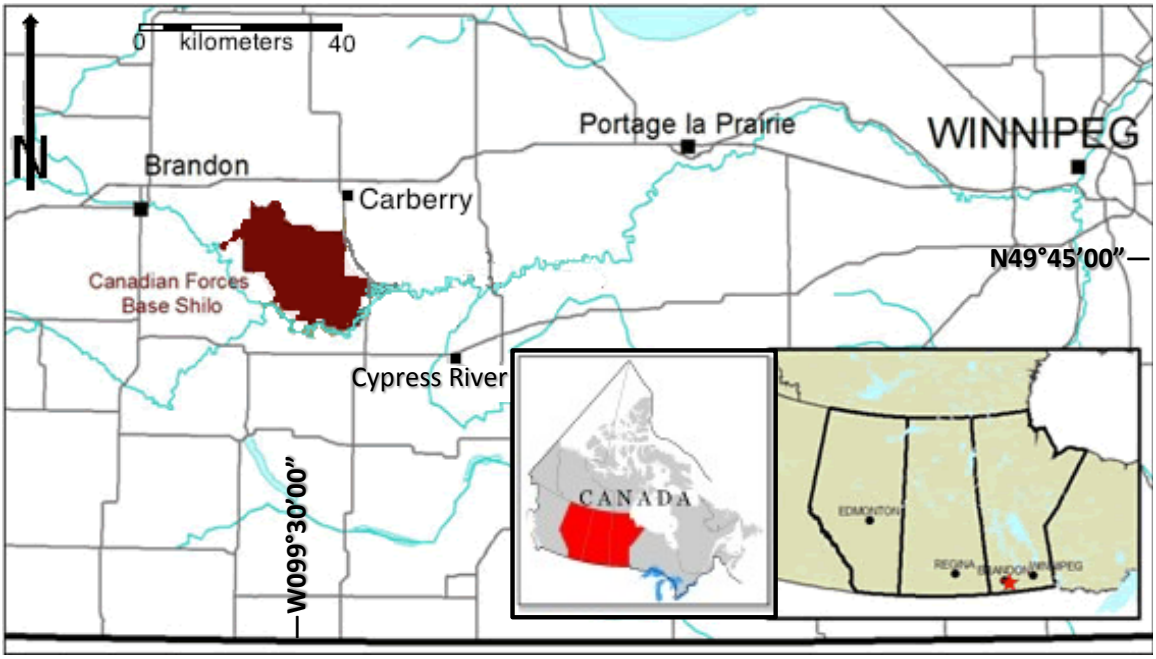

Figure 1 – Location of the study area—Canadian Forces Base Shilo—in southern Manitoba is shown in dark red. Also shown are the locations of the primary weather station (Carberry), and the two secondary weather stations (Brandon, and Cypress River).

Onsite research coupled with LANDSAT analysis (Rowland, 2003) provided optical remotely sensed classification of 10 regions of interest (ROI) within the study area. Further research (Buckley, 2002; 2004; 2008) demonstrated the use of polarimetric SAR-based land cover classification to present eight land cover classes, namely coniferous forests, deciduous forests, marshes, rivers, sand dunes, mixed prairie grasses, bare ground, and bush. It is from this further research by Buckley (2008) that georeferenced digital bitmap masks defining eight ROIs were provided for the current study (Table 1). The exact vegetation state within each of the below noted classifications may vary year on year (such as from the year they were classified to the year of our final image

analyzed) based on such factors as activity within the study area, and regrowth of grasses following burns. Rowland (2003) noted that while grassy classified (herbaceous) areas may vary among themselves (i. e. as the percentage of healthy grass increases, the percentage of poor health grass decreases), the shrub and tree areas were less likely to change vegetation type. As well, the ROI labeled "burn" represents a previously herbaceous area, which was at least partially burned in 2005, and likely, is in a state of partial if not full recovery in our images (2008, 2009, 2011), and therefore should be regarded as a herbaceous ROI.

The types of vegetation in the herbaceous sites are fairly similar to each other with the main difference between the ROIs being the percentage mix of grass cover and bare ground. This is not the case for the shrub and tree ROIs, which have distinctly different vegetation between sites varying from the homogeneous plantation of Scots Pine (pine), to mixed conifer trees with a majority of spruce (conifer), to all deciduous (aspen), and finally a wide mixture of conifer and deciduous (riparian).

Table 1 – Regions of Interest (from Buckley (2004) and Rowland, (2003))

Region of Interest	**Description**	**Area (ha)**	**ROI Grouping**
Healthy Grass	81-100% grass cover	424.3	*Herbaceous*
Medium Health Grass	36-80% grass cover	418.0	*Herbaceous*
Poor Health Grass	10-35% grass cover	507.3	*Herbaceous*
Burn	50% scrub & 50% bare	313.8	*Herbaceous*
Conifer	Mainly spruce	1874.3	*Shrub and tree*
Pine	Plantation of Scots pine	163.9	*Shrub and tree*
Riparian	Dwarf birch, willow, alder, spruce, tamarack	542.8	*Shrub and tree*
Aspen	Aspen	202.3	*Shrub and tree*

Methods

Weather Data and Drought Code Calculation

Daily and hourly weather data was obtained from Environment Canada from 1 January 2007 to 31 December 2012 for the Carberry weather station (Lat/Long 49°54'20.900"N 99°21'26.800"W, Elevation: 383.50 m) located approximately 20km from the centre of the study area (Figure 1). On occasions when this data was absent, data from both Brandon (49°54'00.000" N 99°57'00.000" W, Elevation 409.40m) and Cypress River (49°33'44.000" N 99°04'26.000" W Elevation: 374.00 m) – both of which are approximately 35km from the study area – was obtained and averaged.

Daily Drought Code (DC) values were calculated from these weather data using the noon temperature (in °C) and the total daily precipitation in mm with the equations provided by Van Wagner (1985). Due to the relatively low wintertime precipitation in the study region and the well-drained nature of the soils, these DC calculations were made accounting for the overwintering of the previous season's DC value. As described by Lawson and Armitage (2008), seasons start on the third successive day that noon temperatures of 12°C or higher have been recorded, and end on either 1 November, when snow covers the ground, or freeze up, whichever is earlier. Besides enabling the calculation of DC, these dates also helped selecting the RADARSAT-2 images in the time series that will be used in the study.

SAR Image Collection

A time-series of 82 RADARSAT-2 images in Fine Quad Pol SLC was acquired for CFB Shilo between 16 June 2008 and 7 November 2012 during all seasons and on both the descending and ascending satellite orbits using the same beam mode (FQ18). These FQ18 images have near- and far-range incidence angles from the nadir of 37.4 and 38.9**°,** and nominal resolutions from 8.6 m and 8.3 m, respectively, and a pixel spacing of 4.5 m × 5.1 m (range × azimuth). RADARSAT-2 operates within C-band and transmits and receives at a frequency of 5.405 GHz corresponding to a wavelength of 5.55 cm. Of these original 82 images, 45 images (24 descending and 21 ascending) occur during the DC season noted above; it is from these 24 descending orbit images that the extreme wet and dry days, as well as, the in-season wet day were selected.

DC values for image collection days were calculated to determine the image dates that have both the highest and lowest DC values corresponding to the extreme dry and wet dates, respectively, within the available image time-series. Based on this data, 18 May 2009 was selected as the extreme wet condition acquisition day with a DC value of 22, and 23 October 2011 was determined to be the extreme dry condition day with a DC value of 655. Once these extreme wet/dry conditions were identified, the DC values for images within the same growing season (ie within approximately one month of the extreme conditions) were reviewed to locate the image that was the closest in date to either of the extremes and had the greatest difference in the DC. The image for 14 October 2008 is only 9 days earlier in the season that the extreme dry condition yet has a DC value of 244 making it considerably wetter yet with a similar vegetation state. This

in-season wet and dry comparison will provide some control of differences between the extreme wet and dry conditions due to differing states of vegetation growth. The three selected images are shown in Figure 2 with their parameters described in Table 2.

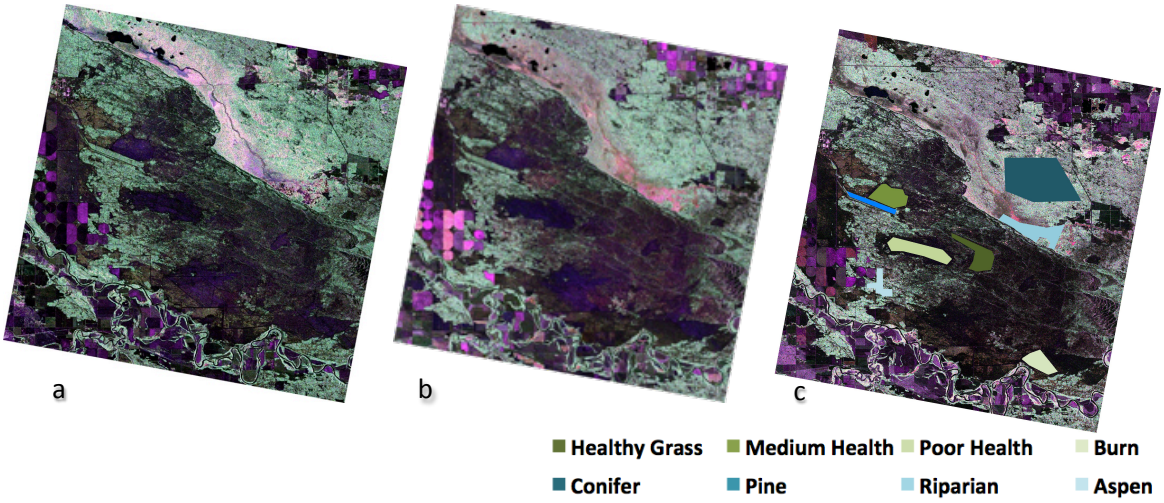

Figure 2 - Orthorectified and Lee filtered RADARSAT-2 polarimetric SAR imagery of CFB Shilo, Manitoba, Canada using Fine Quad Pol mode (FQ18): a. extreme wet condition on 18 May 2009 (DC=22); b. in-season wet condition on 14 October 2008 (DC=244); and c. extreme dry condition on 23 October 2011 (DC=655). Regions of Interest are shown on image c. Image colouration: red channel C-HH, green channel C-HV, blue channel C-VV.

Table 2 – Characteristics of the RADARSAT-2 images used in the study area.

Parameter	Extreme Wet Condition	In-Season Wet Condition	Extreme Dry Condition
Date	18 May 2009	14 October 2008	23 October 2011
Time	12:49:16Z	12:49:08Z	12:49:43Z
Beam Mode	FQ18	FQ18	FQ18
Incidence Angle	38.2°	38.2°	38.2°
Orbit	Descending	Descending	Descending
Precipitation (3-day total)(mm)	3.6	10.2	0.4
Precipitation (7-day total)(mm)	57.6	10.2	0.4
Drought Code	22	244	655

SAR Image Processing and Analysis

The RADARSAT-2 images were analyzed using PCI Geomatica 2014 for all analyses except the van Zyl decomposition. They were first filtered for speckle noise using the Improved Sigma Lee filter which is intended to eliminate the deficiencies in the original Sigma Lee Filter which produced "biased estimation and blurring and depressing strong reflected targets".(Lee et al., 2009, p.202). Orthorectification of the images was conducted using the *Rational Functions Math Model* within Geomatica's OrthoEngine combined with NASA's Shuttle Radar Topographic Mission (SRTM) 3-arcsecond digital

elevation data (DEMs) (Jarvis et al., 2008). ROI bitmasks were then overlaid and the pixel data within each ROI was extracted for numerical analysis. ESA PolSARpro version 4.2 was used to calculate and analyze the van Zyl polarimetric decomposition for the three image dates. Similar to the process in Geomatica, the images were filtered using the Improved Sigma Lee Filter and georeferenced prior to being overlaid by the ROI bitmasks and the data extracted for each ROI.

For the three dates, derivative-images were calculated for all parameters to be analyzed. As summarized in Table 3, both linear (HH, HV, VV) and synthesized circular (LL, LR, RR) backscatter intensities were calculated. Polarimetric decomposition variables were calculated which included the following incoherent decomposition methods: 1) the Freeman-Durden (1998), and van Zyl (2011) decompositions that allow determining mean target surface, double-bounce, and volume scattering; 2) the Cloude-Pottier decomposition (Cloude & Pottier, 1997) with its mean $\boldsymbol{\alpha}$ angle characterizing the dominant scattering mechanism, Entropy ($\boldsymbol{H}$) characterizing the importance of one scattering mechanism over the two others, and Anisotropy ($\boldsymbol{A}$) concerning the mixing of the second and third scatterers. Polarimetric discriminators (Touzi et al., 1992) were also computed, which included: the maximum and minimum of the completely polarized component (d_{max}, d_{min}) and the dynamic range of this degree of polarization (Δd); the maximum and minimum of the received power (Pr_{max}, Pr_{min}) and their normalized ratio, the coefficient of fractional polarization (FP); and the maximum and minimum of the scattered intensity ($S_{max,}$ S_{min}) and their relative normalized dynamic range (ND_s).

Table 3 – Polarimetric parameters and decompositions calculated and analyzed for the three RADARSAT-2 image dates in this study.

Symbol	Parameter and Definition	Reference
C-HH	C-band linear backscatter intensity (horizontal transmit, horizontal receive)	
C-HV	C-band linear backscatter intensity (horizontal transmit, vertical receive)	
C-VV	C-band linear backscatter intensity (vertical transmit, vertical receive)	
C-RR	C-band circular backscatter intensity (right transmit, right receive)	
C-LR	C-band circular backscatter intensity (left transmit, right receive)	
C-LL	C-band circular backscatter intensity (left transmit, left receive)	
CP-*H*	Entropy: characterizing the importance of one scattering mechanism over the two others (index)	Cloude & Pottier, 1997
CP-*A*	Anisotropy: concerning the mixing of the second and third scatterers (index)	Cloude & Pottier, 1997
CP-α	alpha angle: characterizing the dominant scattering mechanism (degree)	Cloude & Pottier, 1997

Symbol	Parameter and Definition	Reference
vZ vol	van Zyl volume scattering. Modelled on three-layered forest consisting of various orientations of dielectric cylinders. In power units.	van Zyl et al., (2011)
vZ surf	van Zyl single bounce. Single reflections from smooth or slightly rough surfaces. In power units.	van Zyl et al., (2011)
vZ dbl	van Zyl double bounce. Modelled as dihedral corner reflector. In power units.	van Zyl et al., (2011)
FD vol	Freeman-Durden volume scattering. Modelled as canopy scatter from randomly oriented very thin cylinder-like scatterers (dipoles). In power units.	Freeman-Durden (1998)
FD surf	Freeman-Durden single bounce. Modelled as first-order Bragg surface scatterer. In power units.	Freeman-Durden (1998)
FD dbl	Freeman-Durden double bounce. Modelled as dihedral corner reflector. In power units.	Freeman-Durden (1998)
$\mathbf{d_{max}}$	The maximum ratio of the intensity in the completely polarized component of an electromagnetic wave to the total intensity in the electromagnetic wave (index).	Touzi et al., (1992)

Symbol	Parameter and Definition	Reference
$\mathbf{d_{min}}$	The minimum ratio of the intensity in the completely polarized component of an electromagnetic wave to the total intensity in the electromagnetic wave (index).	Touzi et al., (1992)
Δd	Dynamic range between maximum and minimum degrees of polarization (index).	Touzi et al., (1992)
$\mathbf{Pr_{max}}$	Maximum of the received power. In power units.	Touzi et al., (1992)
$\mathbf{Pr_{min}}$	Minimum of the received power. In power units.	Touzi et al., (1992)
FP	Coefficient of fractional polarization, the normalized ratio of max to min received power (index).	Touzi et al., (1992)
$\mathbf{S_{max}}$	Maximum of the scattered intensity. In power units.	Touzi et al., (1992)
$\mathbf{S_{min}}$	Minimum of the scattered intensity In power units.	Touzi et al., (1992)
$\mathbf{ND_s}$	Relative normalized dynamic range of max and min scattering intensity (index).	Touzi et al., (1992)

The eight ROIs were imported into Geomatica and PolSARpro and bitmap masks were created for each and overlaid on the calculated images. Linear scale power values for

overlaid pixels were extracted and the median for each of the ROIs was calculated for each parameter. Following the method of Bourgeau-Chavez *et al.* (2013b), the normalized difference (ND) between these median values of corresponding ROIs for each parameter on both the extreme or in-season wet and dry images was calculated with the following equation:

$$\text{Normalized Difference} = \frac{(\text{wet condition} - \text{dry condition})}{\text{wet condition}} * 100\%$$

Where appropriate, the linear power values were also transformed into dB and differences calculated enabling comparison to the minimum required radiometric accuracy limit for RADARSAT-2. Côté *et al.* (2009) note this accuracy is 0.43dB for a single measurement, so the difference between two independent samples must be twice that, or 0.86dB to be radiometrically accurate.

The eight ROIs were combined into their two groups—four each into *herbaceous* and *shrub and tree* (n=4) as shown above in Table 1—and a one-way analysis of variance (ANOVA) was conducted to test whether or not the differences between the two comparisons are statistically significant for the two groupings, as well as a grouping of all eight ROIs (n=8). The ANOVA was run on the four *herbaceous* ROIs in pairs, first between the extreme dry and extreme wet conditions, and then between the extreme dry and in-season wet conditions. The same was done with the *shrub and tree* ROIs, and finally on all eight ROIs as a whole. This analysis was conducted at the 95% confidence

interval, which requires that the null hypothesis (that there is no statistical difference between the data sets) be rejected if the corresponding *p*-value is less than 0.05.

Results

Site by site evaluation

Figures 3 and 4 present the median values for the C-Band linear and synthesized circular backscatter intensities, respectively, in dB for each of the ROIs on the three image dates. Figure 5 shows the normalized percent differences for the linear backscatter intensities parameters for both the extreme wet and dry, and in-season wet and dry comparison, with Figure 6 showing the same for the synthesized circular backscatter intensities. Both linear (HH, HV, VV) and synthesized circular (LL, LR, RR) backscatter intensities show strong differences between the extreme wet and dry days. The differences are greater for *herbaceous* ROIs—typically between 55 and 65%—while for the *shrub and tree* ROIs they are between 25 and 40%. The In-season comparison also shows large differences for the *herbaceous* ROIs for all parameters, generally between 50 and 60%, except for HV which varied from 26 to 48%. The three circular polarizations produced similar differences; for the linear polarizations, HV was much lower while VV was slightly higher than HH. While always greater on the wet day, the *shrub and tree* ROIs had normalized differences much lower, typically less than 25% and as low as 1%—*riparian* was the exception with differences as much as twice as great as this. For the in-season comparison *pine*, *conifer* had all differences and for *aspen*, C-LL and C-RR, below the radiometric accuracy limit; all other parameters were above the accuracy limit.

a. C-HH

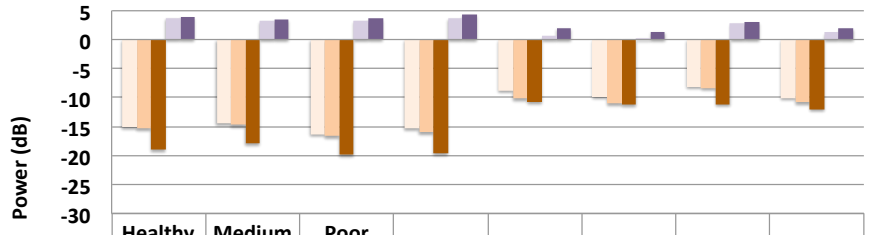

	Healthy Grass	Medium Health	Poor Health	Burn	Conifer	Pine	Riparian	Aspen
Extreme Wet Median (dB)	-15.11	-14.46	-16.31	-15.32	-8.81	-9.89	-8.15	-10.08
In-season Wet Median (dB)	-15.27	-14.72	-16.60	-15.94	-10.19	-11.00	-8.36	-10.84
Extreme Dry Median (dB)	-19.03	-17.93	-19.87	-19.66	-10.82	-11.29	-11.19	-12.04
In-season Difference (dB)	3.76	3.21	3.27	3.72	0.63	0.29	2.84	1.20
Extreme Difference (dB)	3.92	3.47	3.56	4.33	2.01	1.40	3.05	1.96

b. C-HV

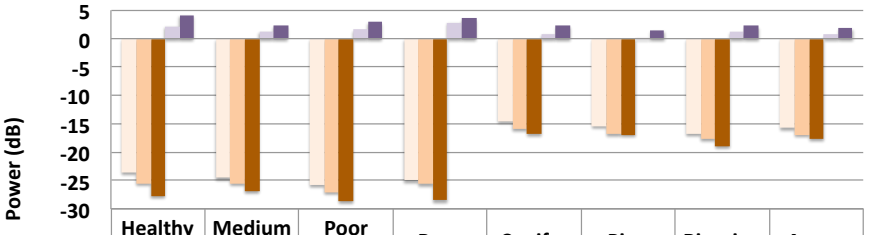

	Healthy Grass	Medium Health	Poor Health	Burn	Conifer	Pine	Riparian	Aspen
Extreme Wet Median (dB)	-23.52	-24.50	-25.70	-24.97	-14.50	-15.38	-16.73	-15.75
In-season Wet Median (dB)	-25.49	-25.52	-27.05	-25.66	-15.94	-16.84	-17.69	-16.92
Extreme Dry Median (dB)	-27.68	-26.84	-28.63	-28.50	-16.80	-16.89	-18.95	-17.64
In-season Difference (dB)	2.19	1.32	1.58	2.85	0.86	0.06	1.26	0.73
Extreme Difference (dB)	4.17	2.34	2.93	3.53	2.31	1.51	2.22	1.90

c. C-VV

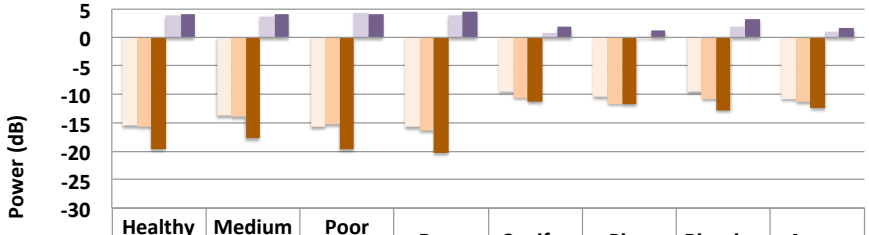

	Healthy Grass	Medium Health	Poor Health	Burn	Conifer	Pine	Riparian	Aspen
Extreme Wet Median (dB)	-15.43	-13.67	-15.62	-15.66	-9.42	-10.44	-9.54	-10.75
In-season Wet Median (dB)	-15.67	-14.00	-15.28	-16.34	-10.58	-11.62	-10.82	-11.35
Extreme Dry Median (dB)	-19.53	-17.72	-19.60	-20.23	-11.32	-11.74	-12.76	-12.42
In-season Difference (dB)	3.86	3.72	4.32	3.88	0.74	0.11	1.94	1.07
Extreme Difference (dB)	4.10	4.05	3.97	4.56	1.90	1.30	3.22	1.68

Figure 3 – ROI median values for C-band linear backscatter intensities (a. C-HH; b. C-HV; c. C-VV) from the extreme wet, in-season wet, and extreme dry images. Differences between the extreme wet and extreme dry, and the in-season wet and extreme dry images for each parameter within each ROI are also presented. All values shown are in dB.

a. C-LL

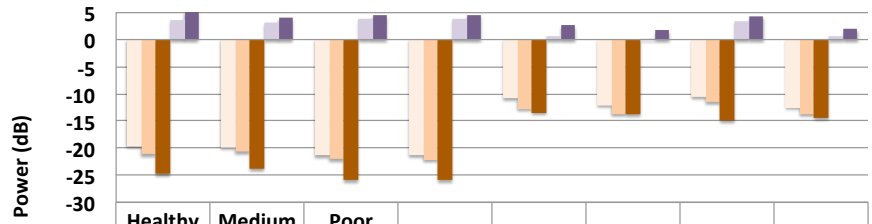

	Healthy Grass	Medium Health	Poor Health	Burn	Conifer	Pine	Riparian	Aspen
Extreme wet median (dB)	-19.59	-19.81	-21.38	-21.30	-10.90	-12.12	-10.63	-12.50
in-season wet median (dB)	-21.16	-20.68	-22.05	-22.08	-12.78	-13.75	-11.58	-13.76
Extreme dry median (dB)	-24.72	-23.77	-25.88	-25.86	-13.48	-13.82	-14.97	-14.45
in-season Difference (dB)	3.56	3.10	3.84	3.78	0.70	0.07	3.38	0.69
Extreme Difference (dB)	5.13	3.96	4.50	4.56	2.58	1.70	4.34	1.95

b. C-LR

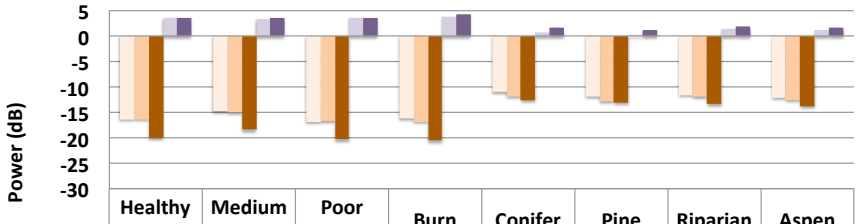

	Healthy Grass	Medium Health	Poor Health	Burn	Conifer	Pine	Riparian	Aspen
Extreme wet median (dB)	-16.34	-14.87	-16.85	-16.22	-11.08	-11.92	-11.63	-12.15
in-season wet median (dB)	-16.31	-15.07	-16.72	-16.79	-11.92	-12.88	-12.01	-12.60
Extreme dry median (dB)	-19.93	-18.43	-20.29	-20.50	-12.63	-13.11	-13.41	-13.77
in-season Difference (dB)	3.63	3.36	3.57	3.72	0.71	0.23	1.40	1.17
Extreme Difference (dB)	3.60	3.56	3.44	4.28	1.56	1.18	1.79	1.62

c. C-RR

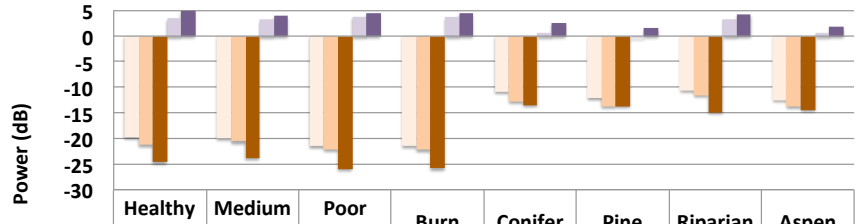

	Healthy Grass	Medium Health	Poor Health	Burn	Conifer	Pine	Riparian	Aspen
Extreme wet median (dB)	-19.73	-19.92	-21.49	-21.44	-10.92	-12.14	-10.64	-12.49
in-season wet median (dB)	-21.21	-20.61	-22.07	-22.16	-12.77	-13.70	-11.54	-13.75
Extreme dry median (dB)	-24.67	-23.80	-25.92	-25.87	-13.50	-13.68	-14.87	-14.42
in-season Difference (dB)	3.47	3.19	3.85	3.71	0.72	-0.02	3.33	0.68
Extreme Difference (dB)	4.95	3.88	4.43	4.43	2.58	1.54	4.23	1.93

Figure 4 – ROI Median values for C-band circular backscatter intensities (a. C-LL; b. C-LR; c. C-RR) from the extreme wet, in-season wet, and extreme dry images. Differences between the extreme wet and extreme dry, and the in-season wet and extreme dry images for each parameter within each ROI are also presented. All values shown are in dB.

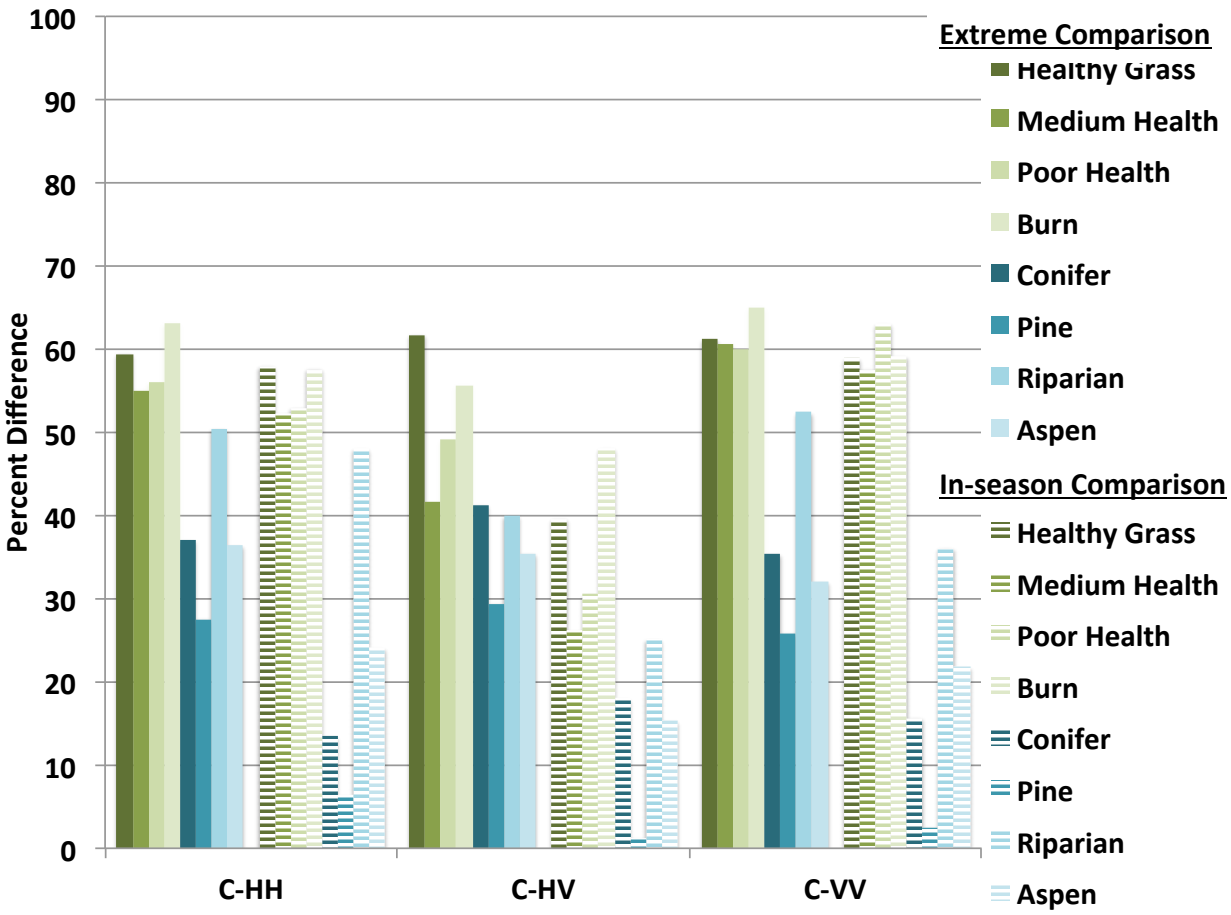

Figure 5 – Normalized percent difference between ROI median values for C-band linear backscatter intensities (C-HH, C-HV, C-VV) for extreme wet and dry, and in-season wet and dry comparisons.

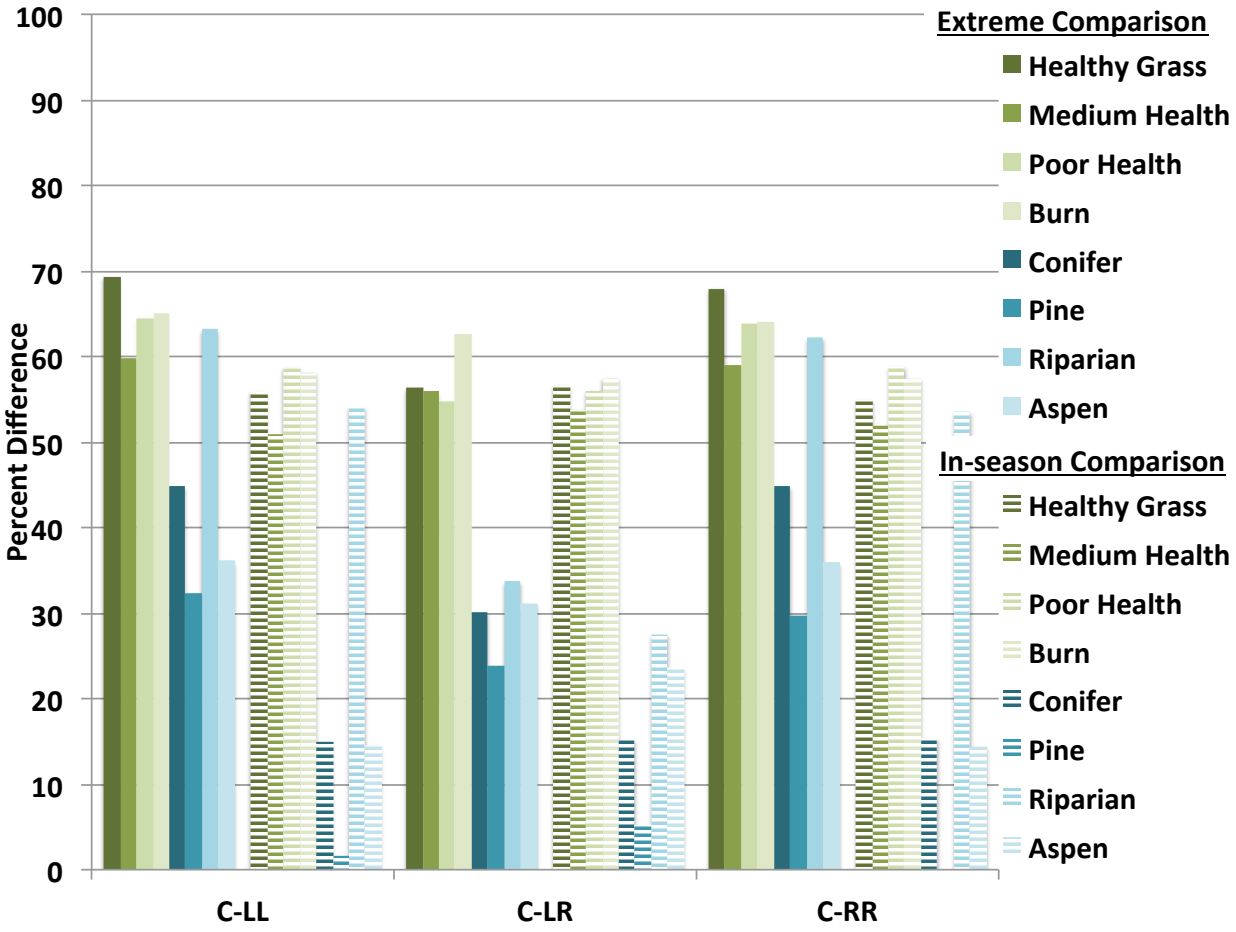

Figure 6 - Normalized percent difference between ROI median values for C-band circular backscatter intensities (C-LL, C-LR, C-RR) for extreme wet and dry, and in-season wet and dry comparisons.

Figure 7 presents the median values in dB for the Freeman-Durden polarimetric decompositions for each ROI on the three dates, with Figure 8 showing the normalized percent difference between these parameters for both the extreme and in-season comparison. Freeman-Durden (FD) decomposition shows large, consistent differences between both the extreme and in-season wet and dry images for the *herbaceous* ROIs. For the extreme comparison, these differences are between approximately 45 and 80 percent, with the in-season comparison ranging from 30 to 82 percent; in both cases double bounce has the greatest (65 to 75%) with single bounce being slightly greater (50 to 60%) than volume. Single and double bounce are both very consistent between the two comparisons. Results are more mixed for the *shrub and tree* ROIs with all negative results for the single bounce in the extreme comparison and half of the results for the in-season being below the radiometric accuracy limit.

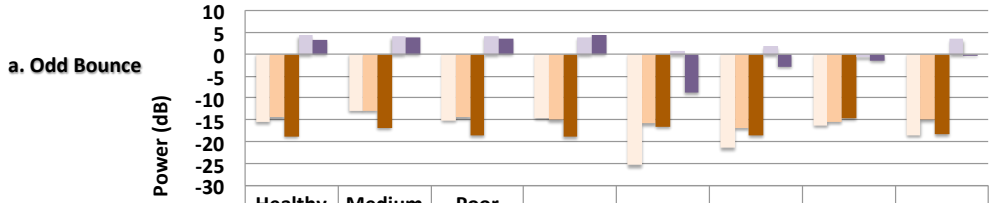

	Healthy Grass	Medium Health	Poor Health	Burn	Conifer	Pine	Riparian	Aspen
Extreme Wet Median (dB)	-15.49	-12.90	-15.05	-14.56	-25.35	-21.41	-16.20	-18.42
In-Season Wet Median (dB)	-14.46	-12.86	-14.44	-15.03	-15.82	-16.76	-15.35	-14.94
Extreme Dry Median (dB)	-18.72	-16.84	-18.58	-18.92	-16.58	-18.58	-14.69	-18.36
In-Season Difference (dB)	4.26	3.98	4.14	3.90	0.76	1.82	-0.67	3.43
Extreme Difference (dB)	3.24	3.94	3.53	4.37	-8.78	-2.83	-1.52	-0.06

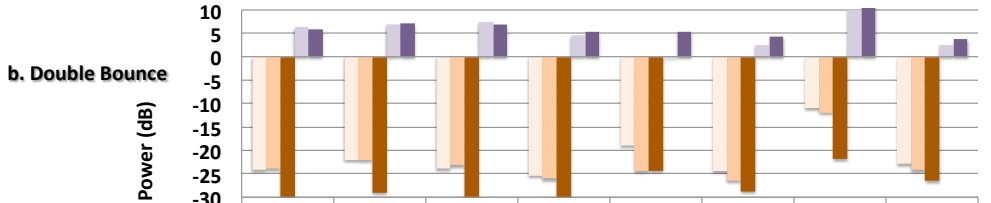

	Healthy Grass	Medium Health	Poor Health	Burn	Conifer	Pine	Riparian	Aspen
Extreme Wet Median (dB)	-24.14	-21.98	-23.88	-25.30	-18.96	-24.35	-11.06	-22.87
In-Season Wet Median (dB)	-23.87	-22.05	-23.20	-26.06	-24.32	-26.36	-11.95	-24.18
Extreme Dry Median (dB)	-30.08	-29.00	-30.64	-30.53	-24.32	-28.73	-21.91	-26.56
In-Season Difference (dB)	6.21	6.96	7.45	4.47	0.00	2.37	9.95	2.38
Extreme Difference (dB)	5.94	7.02	6.77	5.24	5.36	4.37	10.85	3.69

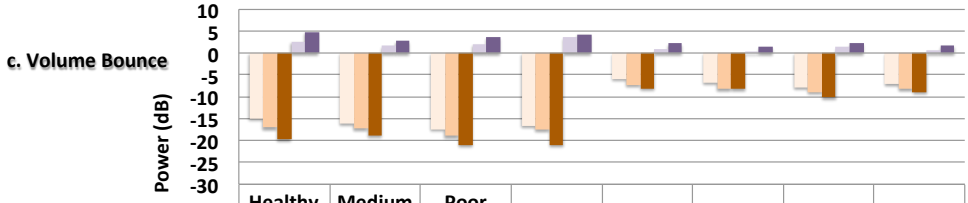

	Healthy Grass	Medium Health	Poor Health	Burn	Conifer	Pine	Riparian	Aspen
Extreme Wet Median (dB)	-14.94	-16.10	-17.35	-16.62	-5.91	-6.77	-7.90	-7.12
In-Season Wet Median (dB)	-17.04	-17.17	-18.88	-17.41	-7.27	-8.25	-8.89	-8.22
Extreme Dry Median (dB)	-19.70	-18.81	-20.94	-20.92	-8.10	-8.27	-10.19	-8.92
In-Season Difference (dB)	2.65	1.63	2.06	3.51	0.83	0.02	1.31	0.70
Extreme Difference (dB)	4.75	2.71	3.59	4.30	2.19	1.49	2.30	1.81

Figure 7 – ROI median values for Freeman-Durden decomposition parameters (a. single bounce; b. double bounce; and c. volume), for the extreme wet and dry, and in-season wet images. Differences between the extreme, and in-season comparisons for each parameter within each ROI are also presented. All values shown are in dB.

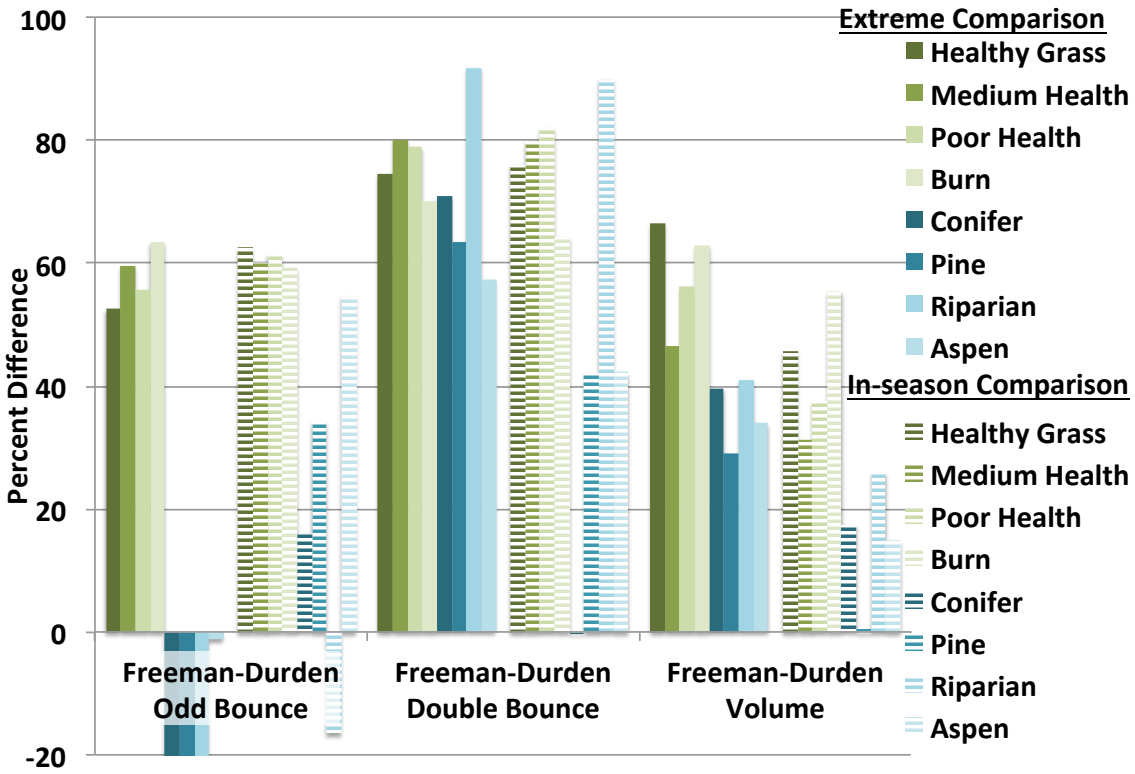

Figure 8 - Normalized percent difference between ROI median values for Freeman-Durden decomposition parameters (odd bounce, double bounce, and volume bounce) for extreme wet and dry, and in-season wet and dry comparisons.

Figure 9 presents the median values in dB for the van Zyl polarimetric decompositions for each ROI on the three dates, while Figure 10 compares the normalized difference between wet and dry days for both the extreme and the in-season comparison. The *herbaceous* ROIs generally have strong differences in both comparisons with odd-bounce being very comparable between the two with differences ranging from about 50 to 65% while double-bounce varied from about 50 to 85%. The difference in volume scatter for the *herbaceous* ROIs was stronger in the extreme condition (56-75%) than in the in-season condition (32-55%). All differences for the *herbaceous* ROIs were above the radiometric accuracy limit. The normalized differences for the *shrub and tree* ROIs where lower than the *herbaceous* ROIs and were generally larger in the extreme condition than the in-season. Double-bounce and volume scatter had the greatest differences in the extreme condition between about 30 and 45%, though riparian was as high as 77%. The radiometric accuracy limit was not met in one third of the *shrub and tree* cases, with pine accounting for half of these.

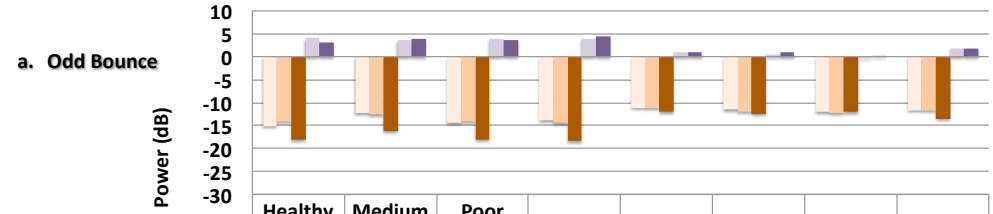

	Healthy Grass	Medium Health	Poor Health	Burn	Conifer	Pine	Riparian	Aspen
Extreme Wet Median (dB)	-15.06	-12.28	-14.42	-13.86	-11.09	-11.57	-12.07	-11.63
In-Season Wet Median (dB)	-13.98	-12.54	-14.04	-14.39	-11.11	-11.90	-12.22	-11.60
Extreme Dry Median (dB)	-18.05	-16.12	-17.99	-18.36	-12.06	-12.41	-12.10	-13.46
In-Season Difference (dB)	4.07	3.58	3.94	3.97	0.95	0.50	-0.12	1.85
Extreme Difference (dB)	3.00	3.85	3.56	4.50	0.97	0.84	0.02	1.82

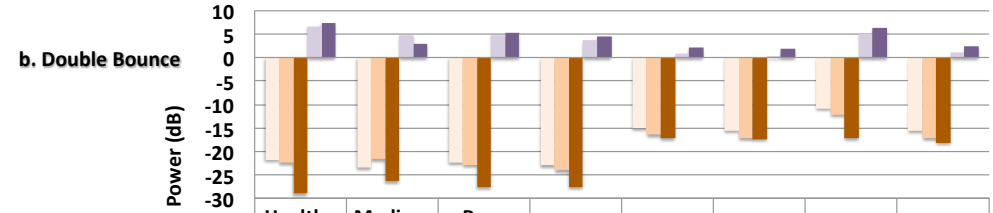

	Healthy Grass	Medium Health	Poor Health	Burn	Conifer	Pine	Riparian	Aspen
Extreme Wet Median (dB)	-21.75	-23.46	-22.39	-22.99	-15.09	-15.57	-10.84	-15.62
In-Season Wet Median (dB)	-22.36	-21.63	-22.80	-23.98	-16.44	-17.16	-12.15	-17.15
Extreme Dry Median (dB)	-29.03	-26.38	-27.61	-27.57	-17.23	-17.39	-17.23	-18.11
In-Season Difference (dB)	6.67	4.75	4.81	3.59	0.79	0.22	5.07	0.96
Extreme Difference (dB)	7.28	2.92	5.22	4.59	2.14	1.82	6.39	2.48

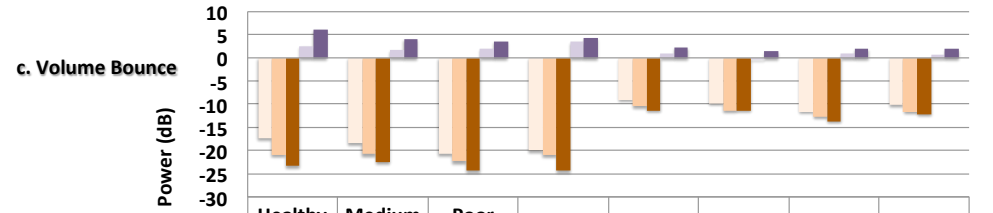

	Healthy Grass	Medium Health	Poor Health	Burn	Conifer	Pine	Riparian	Aspen
Extreme Wet Median (dB)	-17.38	-18.44	-20.75	-20.03	-9.01	-9.79	-11.57	-10.20
In-Season Wet Median (dB)	-20.84	-20.79	-22.34	-20.92	-10.48	-11.37	-12.63	-11.58
Extreme Dry Median (dB)	-23.38	-22.50	-24.37	-24.37	-11.34	-11.31	-13.64	-12.15
In-Season Difference (dB)	2.54	1.71	2.03	3.45	0.87	-0.06	1.00	0.57
Extreme Difference (dB)	6.00	4.06	3.62	4.34	2.33	1.52	2.06	1.94

Figure 9 - ROI median values for Van Zyl decomposition parameter (a. odd bounce; b. double bounce; c. volume) as calculated in PolSARpro, for the extreme wet and dry, and in-season wet images. Differences between the extreme, and in-season comparisons for each parameter within each ROI are also presented. All values shown are in dB.

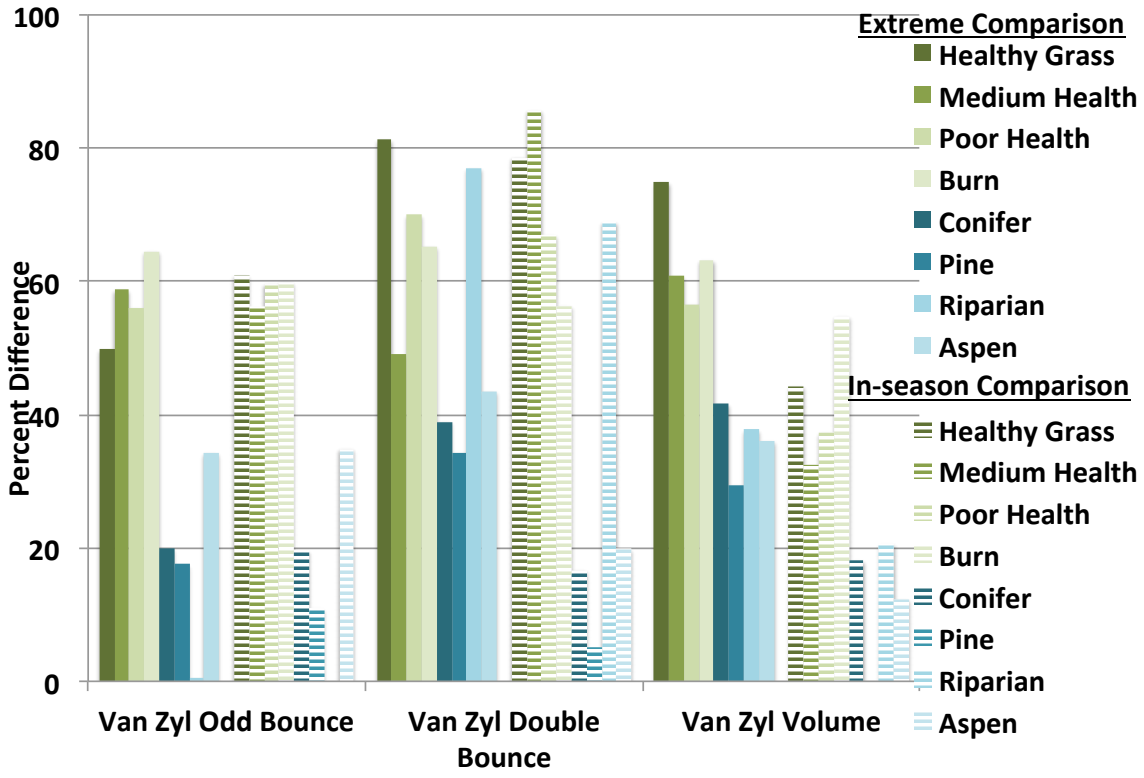

Figure 10 - Normalized percent difference between ROI median values for Van Zyl decomposition parameters (odd bounce, double bounce, and volume bounce) for extreme wet and dry, and in-season wet and dry comparisons.

Figures 11 presents the median values of the Cloude-Pottier (CP) decomposition for each ROI on the three dates; they are shown either in degrees, or as their own indices. Figure 12 shows the normalized percent differences for the CP parameters for the Extreme and In-season comparisons, respectively. For the *herbaceous* ROIs the CP alpha angle generally between 25° and 30° indicates single bounce is the dominant scatterer in these areas while for the *shrub and tree* ROIs the generally 43° to 47° alpha angle shows volume scattering to be dominant; however with the entropy being generally between 0.5 and 0.8 there is a mixture of at least two scattering types for all ROIs. As seen in Figure 12, the CP parameters do not show strong or consistent differences in either wet dry analysis.

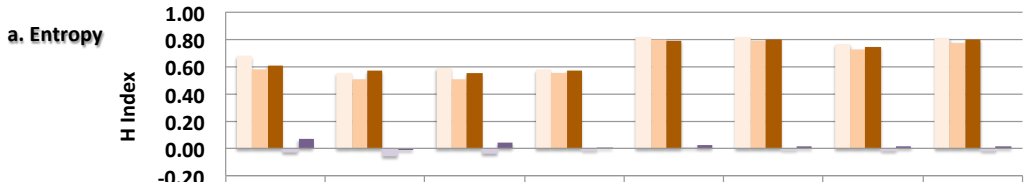

	Healthy Grass	Medium Health	Poor Health	Burn	Conifer	Pine	Riparian	Aspen
Extreme Wet Median	0.68	0.55	0.59	0.58	0.82	0.81	0.76	0.81
In-Season Wet Median	0.58	0.51	0.51	0.55	0.79	0.79	0.73	0.77
Extreme Dry Median	0.61	0.57	0.55	0.57	0.79	0.80	0.75	0.80
In-Season Difference	-0.03	-0.06	-0.04	-0.02	0.00	-0.01	-0.02	-0.02
Extreme Difference	0.07	-0.01	0.04	0.00	0.03	0.01	0.02	0.01

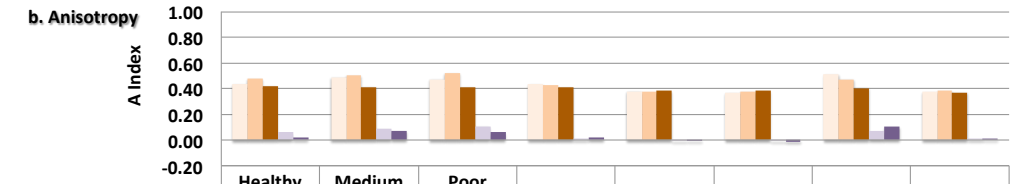

	Healthy Grass	Medium Health	Poor Health	Burn	Conifer	Pine	Riparian	Aspen
Extreme Wet Median	0.44	0.49	0.47	0.43	0.38	0.37	0.51	0.38
In-Season Wet Median	0.48	0.50	0.52	0.42	0.37	0.38	0.47	0.38
Extreme Dry Median	0.42	0.41	0.41	0.41	0.38	0.38	0.40	0.37
In-Season Difference	0.06	0.09	0.11	0.01	-0.01	0.00	0.07	0.01
Extreme Difference	0.02	0.07	0.06	0.02	0.00	-0.01	0.11	0.00

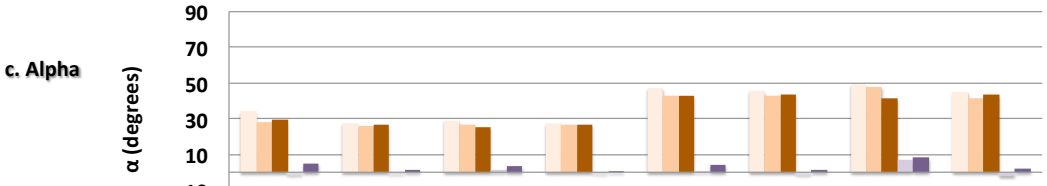

	Healthy Grass	Medium Health	Poor Health	Burn	Conifer	Pine	Riparian	Aspen
Extreme Wet Median	34.06	27.61	29.04	27.30	47.08	45.42	49.22	44.99
In-Season Wet Median	27.99	25.93	26.63	26.54	42.92	42.80	47.76	41.14
Extreme Dry Median	29.10	26.28	25.41	26.82	42.81	43.82	41.13	43.18
In-Season Difference	-1.11	-0.35	1.22	-0.28	0.11	-1.02	6.63	-2.04
Extreme Difference	4.96	1.33	3.63	0.48	4.27	1.61	8.09	1.82

Figure 11 – ROI median values for C-band Cloude-Pottier decomposition parameters (a. Entropy; b. Anisotropy; c. Alpha) from the extreme wet, in-season wet, and extreme dry images. Differences between the extreme, and in-season comparisons for each parameter within each ROI are also presented.

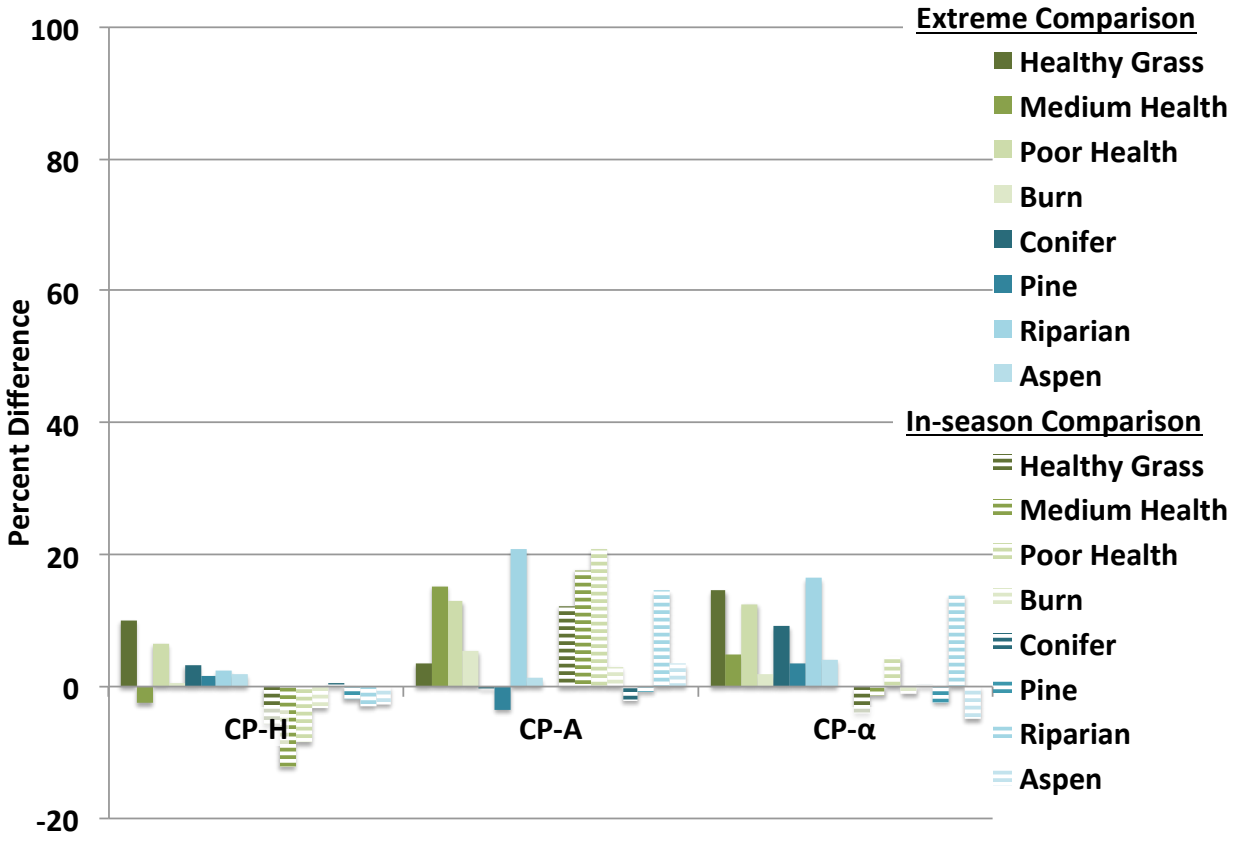

Figure 12 - Normalized percent difference between ROI median values for Cloude-Pottier decomposition parameters (Entropy, Anisotropy, Alpha) for extreme wet and dry, and in-season wet and dry comparisons.

Figures 13, 14, and 15 present the median values for the nine polarimetric discriminators for each of the ROIs, with Figures 16, 17, and 18 showing their normalized percent differences for the extreme and in-season comparisons. Of the nine polarimetric discriminators examined, only the extrema of the power received and the scattered wave intensity show large and consistent differences in either of the comparisons. In the extreme wet and dry comparison the *herbaceous* ROIs usually differed between 50 and 60%, while in the *shrub and tree* ROIs the differences are smaller, usually between about 30-40% except for riparian which is closer to 50%. The in-season comparison also shows strong consistent parameters differences in the *herbaceous* ROIs usually around 55%, except Pr_{min} which is closer to ~38%. For the *shrub and tree* ROIs, the differences are again smaller and more variable, with riparian having greatest difference. The dB differences for pine in both comparisons, and for conifer in the in-season are below the radiometric accuracy limit.

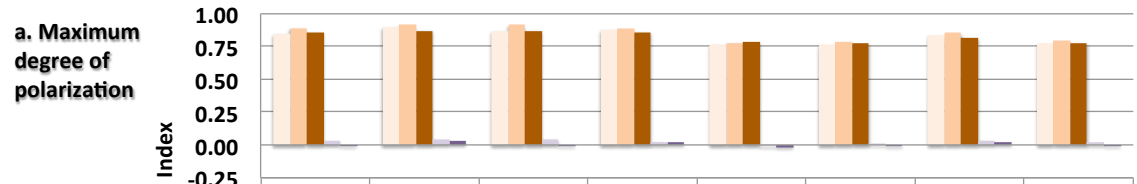

	Healthy Grass	Medium Health	Poor Health	Burn	Conifer	Pine	Riparian	Aspen
Extreme Wet Median	0.85	0.90	0.87	0.88	0.77	0.76	0.84	0.77
In-season Wet Median	0.89	0.91	0.91	0.88	0.78	0.78	0.85	0.79
Extreme Dry Median	0.86	0.87	0.87	0.86	0.78	0.77	0.82	0.78
In-Season Difference	0.03	0.04	0.04	0.02	0.00	0.01	0.04	0.02
Extreme Difference	-0.01	0.03	0.00	0.02	-0.02	-0.01	0.02	0.00

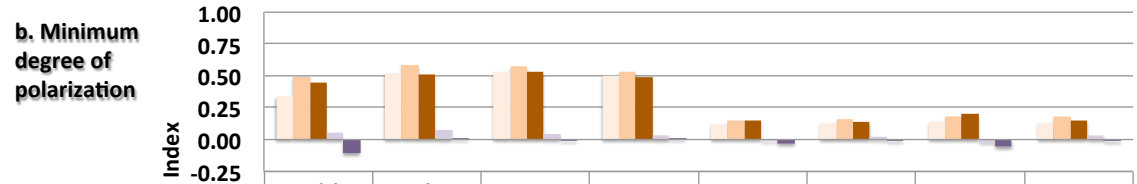

	Healthy Grass	Medium Health	Poor Health	Burn	Conifer	Pine	Riparian	Aspen
Extreme Wet Median	0.34	0.52	0.53	0.50	0.12	0.13	0.14	0.13
In-season Wet Median	0.49	0.58	0.57	0.53	0.15	0.16	0.18	0.18
Extreme Dry Median	0.44	0.51	0.53	0.49	0.15	0.14	0.20	0.15
In-Season Difference	0.05	0.07	0.04	0.03	0.00	0.02	-0.02	0.03
Extreme Difference	-0.11	0.01	0.00	0.00	-0.03	-0.01	-0.06	-0.01

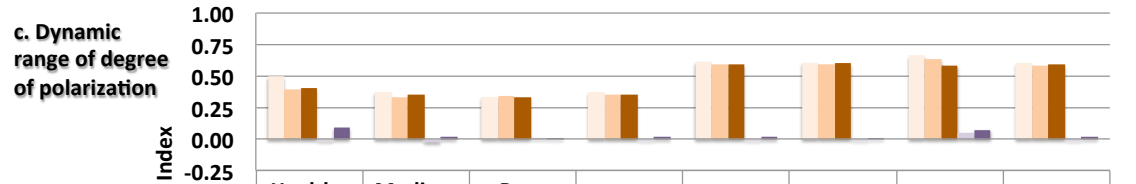

	Healthy Grass	Medium Health	Poor Health	Burn	Conifer	Pine	Riparian	Aspen
Extreme Wet Median	0.49	0.37	0.33	0.37	0.61	0.60	0.66	0.60
In-season Wet Median	0.39	0.33	0.34	0.35	0.59	0.59	0.63	0.58
Extreme Dry Median	0.40	0.35	0.33	0.35	0.59	0.60	0.59	0.59
In-Season Difference	-0.01	-0.03	0.00	-0.01	0.00	-0.01	0.04	-0.01
Extreme Difference	0.09	0.02	0.00	0.02	0.02	0.00	0.07	0.01

Figure 13 - ROI median values for C-band polarimetric discriminators (a. d_{max}; b. d_{min}; and c. Δd) from the extreme wet, in-season wet, and extreme dry images. Differences between the extreme, and in-season comparisons for each parameter within each ROI are also presented.

a. Maximum of the received power (Pr_{max})

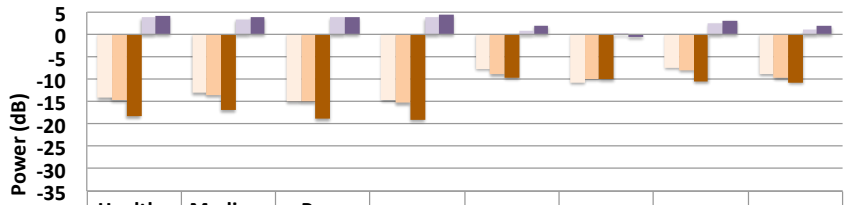

	Healthy Grass	Medium Health	Poor Health	Burn	Conifer	Pine	Riparian	Aspen
Extreme Wet Median (dB)	-14.25	-13.14	-15.07	-14.63	-7.67	-10.74	-7.43	-8.89
In-season Wet Median (dB)	-14.58	-13.50	-14.99	-15.28	-8.97	-9.85	-7.98	-9.72
Extreme Dry Median (dB)	-18.30	-16.91	-18.84	-19.01	-9.65	-10.11	-10.55	-10.71
In-Season Difference (dB)	3.72	3.42	3.85	3.73	0.68	0.26	2.56	0.99
Extreme Difference (dB)	4.05	3.78	3.77	4.37	1.98	-0.62	3.12	1.82

b. Minimum of the received power (Pr_{min})

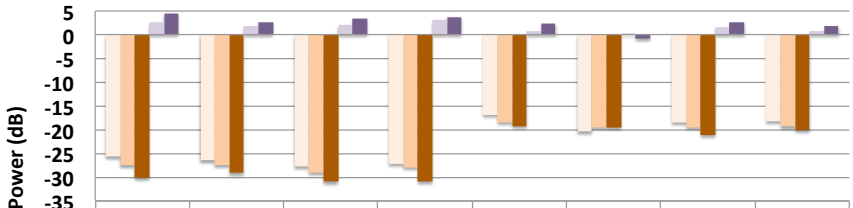

	Healthy Grass	Medium Health	Poor Health	Burn	Conifer	Pine	Riparian	Aspen
Extreme Wet Median (dB)	-25.67	-26.47	-27.73	-27.12	-16.88	-20.44	-18.49	-18.25
In-season Wet Median (dB)	-27.53	-27.46	-29.01	-27.89	-18.46	-19.48	-19.49	-19.43
Extreme Dry Median (dB)	-30.13	-29.15	-30.99	-30.88	-19.24	-19.55	-21.14	-20.13
In-Season Difference (dB)	2.60	1.69	1.98	2.99	0.78	0.07	1.65	0.70
Extreme Difference (dB)	4.46	2.67	3.26	3.76	2.36	-0.89	2.65	1.88

c. Coefficient of Fractional Polarization

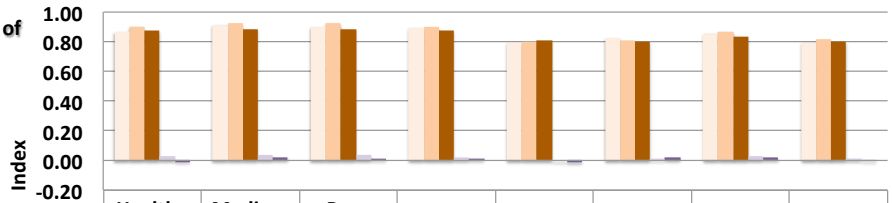

	Healthy Grass	Medium Health	Poor Health	Burn	Conifer	Pine	Riparian	Aspen
Extreme Wet Median	0.86	0.91	0.90	0.89	0.79	0.82	0.85	0.79
In-season Wet Median	0.90	0.92	0.92	0.90	0.80	0.80	0.87	0.81
Extreme Dry Median	0.87	0.89	0.89	0.88	0.80	0.80	0.84	0.80
In-Season Difference	0.03	0.04	0.04	0.02	0.00	0.01	0.03	0.01
Extreme Difference	-0.01	0.02	0.01	0.01	-0.02	0.02	0.02	-0.01

Figure 14 - ROI median values for C-band polarimetric discriminators (a. Pr_{max}; b. Pr_{min}; and c. FP) from the extreme wet, in-season wet, and extreme dry images. Differences between the extreme, and in-season comparisons for each parameter within each ROI are also presented.

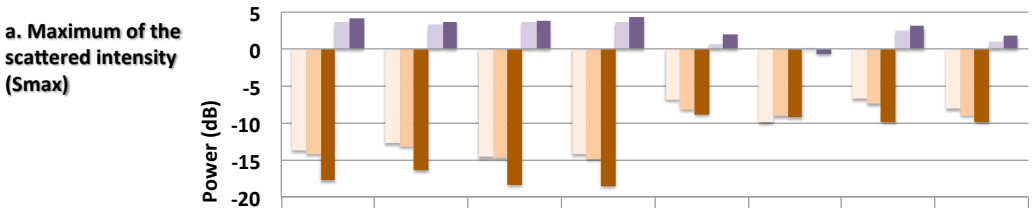

	Healthy Grass	Medium Health	Poor Health	Burn	Conifer	Pine	Riparian	Aspen
Extreme Wet Median (dB)	-13.68	-12.74	-14.63	-14.18	-6.86	-9.96	-6.79	-8.12
In-season Wet Median (dB)	-14.16	-13.15	-14.65	-14.83	-8.20	-9.11	-7.46	-8.98
Extreme Dry Median (dB)	-17.79	-16.43	-18.36	-18.51	-8.88	-9.30	-9.91	-9.89
In-Season Difference (dB)	3.62	3.27	3.70	3.68	0.68	0.19	2.44	0.91
Extreme Difference (dB)	4.10	3.69	3.72	4.33	2.02	-0.66	3.12	1.77

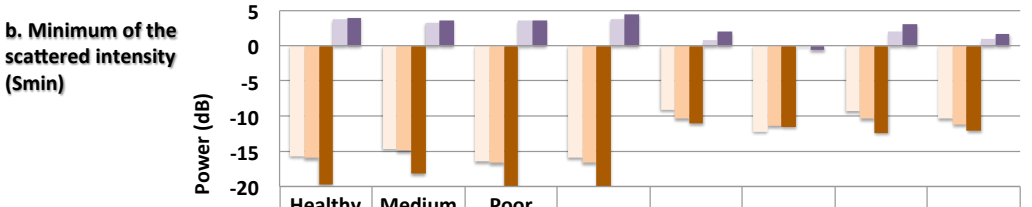

	Healthy Grass	Medium Health	Poor Health	Burn	Conifer	Pine	Riparian	Aspen
Extreme Wet Median (dB)	-15.68	-14.61	-16.49	-15.91	-9.11	-12.17	-9.34	-10.41
In-season Wet Median (dB)	-15.95	-14.93	-16.65	-16.57	-10.36	-11.38	-10.39	-11.17
Extreme Dry Median (dB)	-19.66	-18.22	-20.14	-20.35	-11.07	-11.53	-12.36	-12.10
In-Season Difference (dB)	3.72	3.28	3.49	3.78	0.71	0.15	1.97	0.93
Extreme Difference (dB)	3.98	3.61	3.65	4.43	1.96	-0.64	3.02	1.69

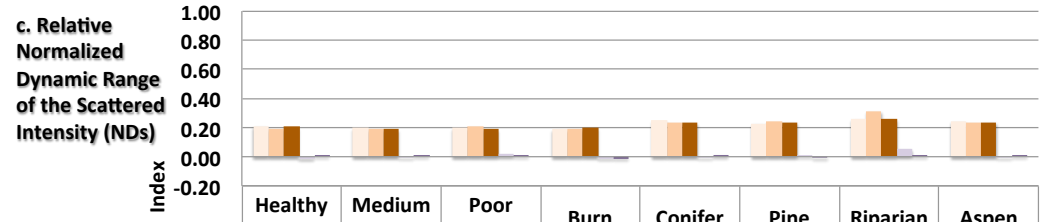

	Healthy Grass	Medium Health	Poor Health	Burn	Conifer	Pine	Riparian	Aspen
Extreme Wet Median	0.21	0.20	0.20	0.19	0.25	0.23	0.26	0.24
In-season Wet Median	0.19	0.19	0.21	0.19	0.23	0.24	0.31	0.23
Extreme Dry Median	0.20	0.19	0.19	0.20	0.23	0.24	0.26	0.24
In-Season Difference	-0.01	0.00	0.02	-0.01	0.00	0.00	0.05	0.00
Extreme Difference	0.01	0.01	0.01	-0.01	0.01	-0.01	0.00	0.01

Figure 15 - ROI median values for C-band polarimetric discriminators (a. S_{max}; b. S_{min}; and c. NDs) from the extreme wet, in-season wet, and extreme dry images. Differences between the extreme, and in-season comparisons for each parameter within each ROI are also presented.

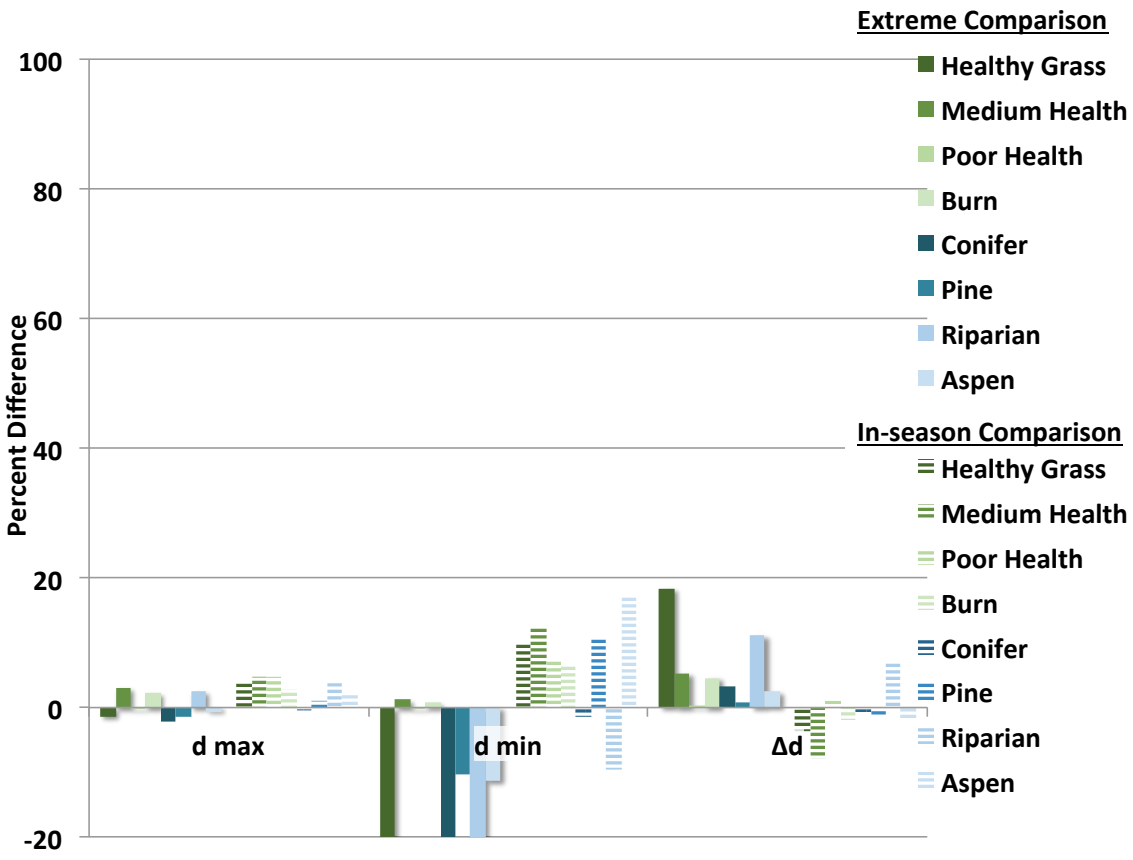

Figure 16 - Normalized percent difference between ROI median values for the C-band polarimetric discriminators maximum and minimum of the degree of polarization, and the degree of polarization dynamic range for extreme wet and dry, and in-season wet and dry comparisons.

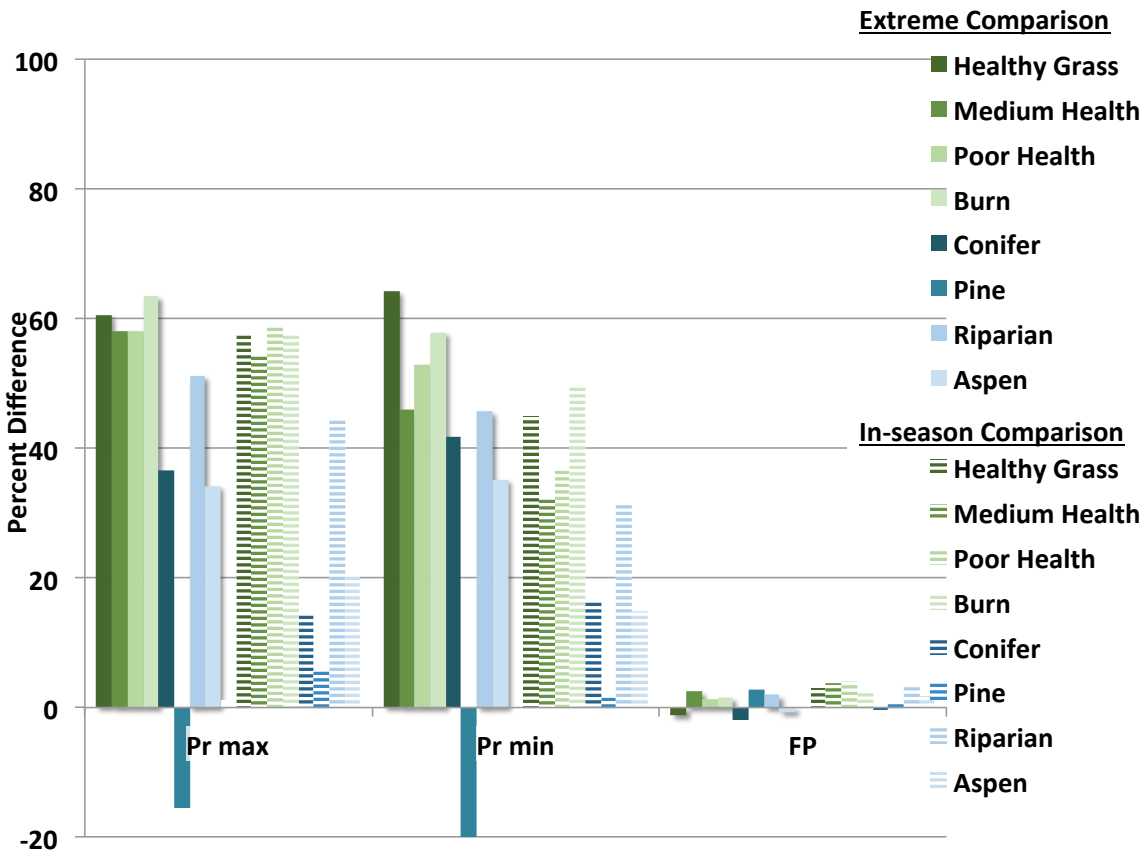

Figure 17 - Normalized percent difference between ROI median values for the C-band polarimetric discriminators maximum and minimum power received, and the coefficient of fractional polarization for extreme wet and dry, and in-season wet and dry comparisons.

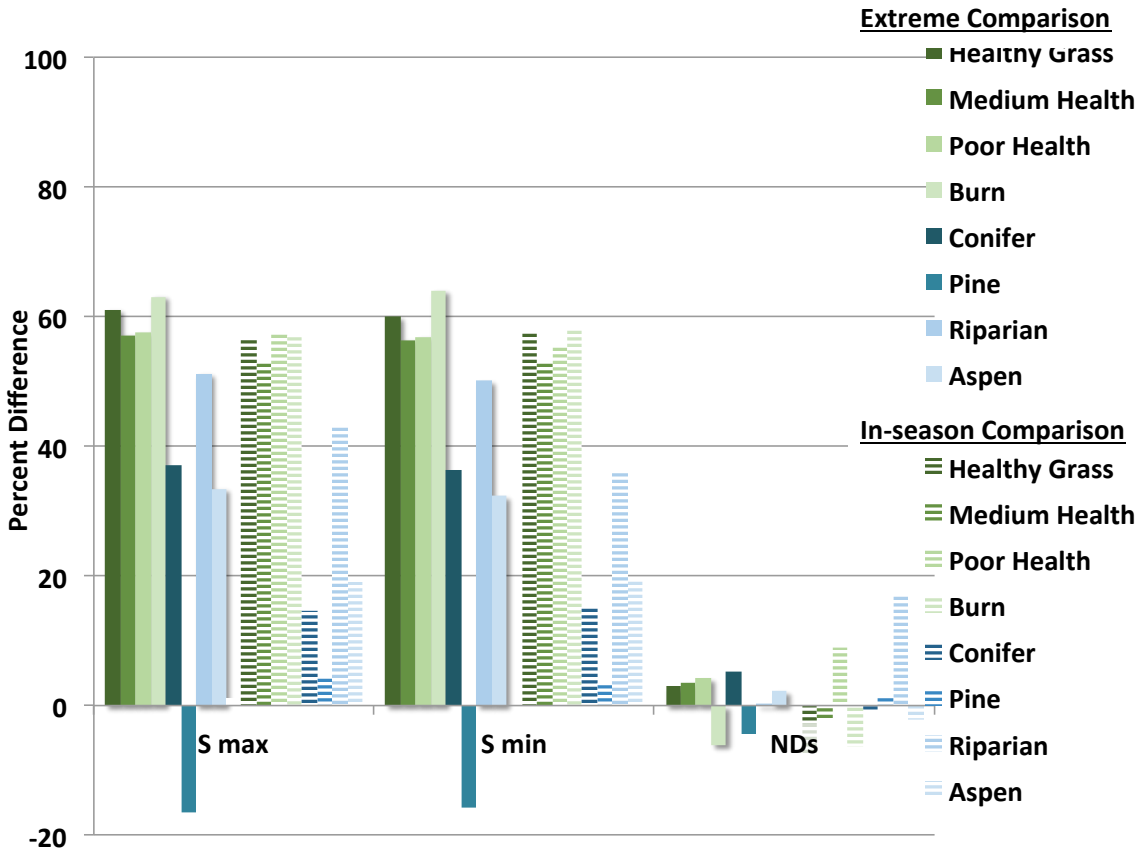

Figure 18 - Normalized percent difference between ROI median values for the C-band polarimetric discriminators maximum and minimum scattering intensities, and the relative normalized dynamic range of maximum and minimum scattering intensity for extreme wet and dry, and in-season wet and dry comparisons.

Overall evaluation across all sites

The normalized differences were calculated for the *herbaceous* and *shrub and tree* grouped ROIs by taking the median of the four associated parameter medians and then using the same normalized difference calculation shown above for each comparison. The same was done for all eight ROIs grouped together. Table 4 presents these results.

Table 4 - Percent normalized differences between grouped ROIs (*n*=4, and *n*=8) parameter medians for each of the investigated polarimetric parameters for both the extreme wet and dry, and in-season wet and dry comparisons.

	Extreme Wet and Dry			**In-season Wet and Dry**		
Parameter	***Herbaceous*** **(*n* =4)**	***Shrub & Tree*** **(*n* =4)**	**All ROIs (*n* =8)**	***Herbaceous*** **(*n* =4)**	***Shrub & Tree*** **(*n* =4)**	**All ROIs (*n* =8)**
C-HH	61.2	35.8	41.4	57.8	15.6	30.5
C-HV	53.7	32.3	42.4	43.6	8.3	25.3
C-VV	60.5	38.4	45.0	61.0	20.4	35.7
C-RR	65.5	44.4	45.1	56.5	17.3	27.8
C-LR	58.6	29.0	39.8	56.3	19.8	31.9
C-LL	66.6	45.8	46.3	57.1	18.5	28.8
CP-*H*	2.1	2.4	6.0	-7.3	-1.5	-4.1
CP-*A*	9.2	-0.8	6.3	15.8	0.0	9.1
CP-α	6.3	7.0	11.2	0.1	-0.3	-1.6

	Extreme Wet and Dry			In-season Wet and Dry		
Parameter	***Herbaceous*** **(*n* =4)**	***Shrub & Tree*** **(*n* =4)**	**All ROIs (*n* =8)**	***Herbaceous*** **(*n* =4)**	***Shrub & Tree*** **(*n* =4)**	**All ROIs (*n* =8)**
vZ volume	66.0	32.9	44.3	49.5	5.7	22.2
vZ surface	59.2	13.8	42.7	60.3	10.8	39.9
vZ double	67.7	36.7	47.9	68.5	11.5	31.9
FD volume	59.4	31.5	44.0	49.6	7.7	27.0
FD surface	58.8	-69.2	45.6	62.0	33.9	55.2
FD double	76.5	66.9	72.0	79.0	21.5	67.2
$\mathbf{d_{max}}$	1.2	-1.4	0.6	4.2	1.0	3.5
$\mathbf{d_{min}}$	1.1	-16.0	-34.5	8.6	10.1	4.7
Δd	5.0	3.0	9.7	-3.2	0.0	-2.3
$\mathbf{Pr_{max}}$	61.3	38.2	20.8	58.1	20.5	28.9
$\mathbf{Pr_{min}}$	57.4	28.6	24.3	47.3	8.3	31.7
FP	1.4	0.6	0.3	3.4	0.9	2.9
$\mathbf{S_{max}}$	61.5	38.9	19.0	57.0	20.8	27.0
$\mathbf{S_{min}}$	61.1	36.4	23.2	56.8	21.4	30.3
$\mathbf{ND_s}$	1.3	3.3	-0.2	-3.3	-0.3	0.5

Analyses were then conducted using the data combined into the two grouped ROIs: *herbaceous*, *shrub and tree,* and All ROIs. As described above, a one-way ANOVA was conducted to test whether or not the differences between the two comparisons are statistically significant for these two n=4 groupings, as well as a grouping of all eight ROIs (n=8). With this analysis being conducted at the 95% confidence level, the p-value must be less than 0.05 for the difference to have statistical significance. Table 4 presents the results of the ANOVA in the form of p-values.

Table 5 - *P*-value of one-way ANOVA for the difference between the extreme wet and dry dates, and for the in-season wet and dry dates for the herbaceous ROIs, shrub and tree ROIs, and all ROIs combined. The non-significant p values are highlighted in ***bold italic***.

	Extreme Wet and Dry			**In-season Wet and Dry**		
Parameter	***Herbaceous* (*n*=4)**	***Shrub & Tree* (*n* =4)**	**All ROIs (*n* =8)**	***Herbaceous* (*n* =4)**	***Shrub & Tree* (*n* =4)**	**All ROIs (*n* =8)**
C-HH	0.0009	0.0130	***0.1591***	0.0018	***0.1435***	***0.2988***
C-HV	0.0040	0.0263	***0.3146***	0.0112	***0.2770***	***0.6809***
C-VV	0.0034	0.0056	***0.1123***	0.0039	***0.0528***	***0.2448***
C-RR	0.0016	0.0065	***0.2023***	0.0016	***0.1210***	***0.4699***
C-LR	0.0025	0.0044	***0.1376***	0.0024	0.0396	***0.2378***
C-LL	0.0014	0.0062	***0.1902***	0.0012	***0.1136***	***0.4601***

	Extreme Wet and Dry			In-season Wet and Dry		
Parameter	***Herbaceous*** **(*n*=4)**	***Shrub & Tree*** **(*n* =4)**	**All ROIs (*n* =8)**	***Herbaceous*** **(*n* =4)**	***Shrub & Tree*** **(*n* =4)**	**All ROIs (*n* =8)**
CP-*H*	***0.4488***	***0.3444***	***0.7182***	***0.1180***	***0.5390***	***0.6776***
CP-*A*	0.0175	***0.5093***	***0.1157***	0.0187	***0.4979***	***0.0722***
CP-α	***0.1884***	0.0123	***0.4809***	***0.8893***	***0.5712***	***0.9305***
vZ volume	0.0106	0.0389	***0.3024***	0.0053	***0.4217***	***0.7301***
vZ surface	0.0098	0.0456	***0.0790***	0.0021	***0.0874***	***0.0730***
vZ double	0.0004	***0.1223***	***0.1758***	0.0011	***0.2614***	***0.2158***
FD volume	0.0041	0.0209	***0.3210***	0.0091	***0.2638***	***0.6823***
FD surface	0.0080	***0.2199***	***0.3363***	0.0028	***0.2931***	0.0030
FD double	0.0038	***0.2749***	***0.1977***	0.0050	***0.3616***	***0.2422***
d_{max}	***0.4595***	***0.8905***	***0.9032***	0.0067	***0.4944***	***0.3432***
d_{min}	***0.6380***	***0.0734***	***0.7782***	***0.1235***	***0.6599***	***0.7754***
Δd	***0.4338***	***0.0884***	***0.6445***	***0.6136***	***0.6489***	***0.9686***
Pr_{max}	0.0016	***0.0855***	***0.2183***	0.0018	***0.0789***	***0.3123***
Pr_{min}	0.0025	***0.1200***	***0.3767***	0.0057	***0.1518***	***0.6348***
FP	***0.4009***	***0.8090***	***0.7613***	0.0072	***0.5291***	***0.3845***
S_{max}	0.0014	***0.0839***	***0.2372***	0.0018	***0.0708***	***0.3552***
S_{min}	0.0014	***0.0837***	***0.2218***	0.0022	***0.0535***	***0.3481***
ND_s	***0.6756***	***0.7980***	***0.8569***	***0.6739***	***0.5505***	***0.7839***

The *herbaceous* ROIs generally show statistically significant differences for both comparisons for most parameters. The linear and circular backscatters and all Freeman-Durden and van Zyl parameters reject the null hypothesis, as do all polarimetric discriminators except the normalized dynamic range in scattering intensity and the fractional polarization. Anisotropy is the only Cloude-Pottier parameter which rejects the null in both comparisons; the remaining parameters either do not, or have mixed results. The *shrub and tree* ROIs show mixed results regarding the ANOVA. Linear and circular backscatter reject the null hypothesis in the extreme comparison, but accept it in the in-season analysis (except C-LR which rejects). Freeman-Durden volume scattering shows statistical differences in the extreme comparison, while the d_{min} discriminator does for both. When all sites are combined there are only two statistically significant differences: d_{min} discriminator being in both comparisons, and Freeman-Durden single bounce in the in-season analysis.

Discussion

Co-polarized linear backscatters (C-VV, and C-HH) provide strong, statistically significant differences (61%) for the *herbaceous* ROIs, with C-HV showing a smaller (54%), but still significant difference. Numerous authors, such as Ulaby *et al.* (1982) and Van der Sanden (2004) note HH and VV as the C-band preferred polarizations for soil moisture mapping, with Sokol *et al.* (2004) also concluding this for soil moisture correlation in bare agricultural fields in Manitoba using similar incidence angles, as well as Bourgeau-Chavez *et al.* (2013) when comparing extreme wet and dry conditions using 20° incidence angle over recently burned and unburned boreal Alaskan sites. In contrast, Kong *et al.* (2014)—using a slightly lower incidence angle (35°) over *Lowveld* South African savannah—and Chen (2013)—using 21° incidence angle over burned and unburned peat bog in Alberta—all found C-HV had either greater wet/dry differences or better soil moisture correlation than C-HH and C-VV. The lower differences for C-HV in this study are also consistent with Wang *et al.*'s (2000) simulations which show C-HV being more dominated by the volume scatter in the biomass which would have a greater differential effect in the seasonal vegetation variation in the extreme dates comparison. Interestingly, for the *herbaceous* ROIs in the extreme and in-season comparisons, C-VV showed very little change between the two comparisons (60.5 and 61.0%, respectively) apparently indicating it was least susceptible to changes in the vegetation state; this is somewhat unexpected as C-VV polarization is usually predicted to be dominated by vegetation scattering especially at shallower incidence angles like the 38° in this study (van Zyl & Kim, 2011). For the combined *shrub and tree* ROIs, linear backscatter showed smaller but still significant differences in the extreme comparison of between 32

and 38% with C-HH and C-VV being greater than C-HV, while the in-season comparison did not produce any statistically significant differences.

All circular backscatter (C-LL, C-LR, C-RR) intensities show strong, significant differences for the *herbaceous* ROIs in both comparisons with all three being approximately 57% in the in-season comparison, and C-RR and C-LL being higher (~66%) than C-LR (59%) in the extreme comparison. Kong *et al.* (2014) had similar findings in their *herbaceous* sites, while Bourgeau-Chavez *et al.* (2013) found C-LR to have the greatest difference in sites with sparse forest canopy and lower biomass. For the *shrub and tree* ROIs, differences in the extreme comparison for C-RR and C-LL are again higher (~45%) than for C-LR (29%), though in the in-season comparison, only C-LR has a statistically significant difference (of 20%). While slightly lower overall than the cross-pol differences, the current study's C-LR difference shows a greater robustness to effects of vegetation with a decrease of only 2% from the extreme to the in-season comparisons for the *herbaceous* ROIs, in contrast to C-LL and C-RR which show a 9% decrease between the two comparisons, and for the *shrub and tree* ROI it is the only circular backscatter to be significant in both comparisons.

As anticipated due to its nature, the Cloude-Pottier decomposition parameters are not suitable for use distinguishing between wet and dry soil conditions as represented by Drought Code in either the *herbaceous* or *shrub and tree* sites as most of the normalized differences do not have statistical significance (CP-*A* being the exception for *herbaceous* ROIs in both comparisons, though the differences are less than 16%). Kong *et al.* (2014)

and Bourgeau-Chavez *et al.* (2013) also found these parameters to be not suited to this task in their study ecosystems, noting them better suited to representing more time-invariant variable such as biomass and surface roughness. Pasolli *et al.* (2011) also found reduced capability of these parameters, attributing at least part of the cause to the variability in their local incidence angles as they investigated highly heterogeneous alpine pastures and meadows.

Similar to others (Kong et al., 2014; Bourgeau-Chavez, et al., 2013a), within the *herbaceous* ROIs, both Freeman-Durden and van Zyl decompositions show strong, statistically significant differences (50-79% and 50-69%, respectively) for all three parameters in both comparisons with double-bounce having the greatest. For both decompositions the volume scattering difference is greater in the extreme comparison (59 and 66%) than the in-season (50 and 50%), while surface- and double-bounce are slightly greater in the in-season (by approximately 1-3%); this implies the effects of the seasonal difference in vegetation state, and the greater attenuation by the vegetation of the single- and double-bounce returns for our higher incidence angle (van Zyl et al., 2011). For the *shrub and tree* ROIs, none of the parameters—with the exception of the two volume scatter results in the extreme comparison—showed a statistically significant difference; this likely a result of the large variability between the differences of individual ROIs within this grouping.

Considering the polarimetric discriminators, Pr_{max}, and to a slightly lesser extent, Pr_{min}; and both S_{max} and S_{min} have strong, significant differences between both the extreme (57-

62%) and in-season (47-58%) moisture conditions in the *herbaceous* ROIs, which are similar to the *herbaceous* results of Kong *et al.* (2014). Of the remaining discriminators d_{max} and d_{min} and their dynamic range, **Δ**d; NDs, and FP, only d_{max} and FP have statistically significant differences for the *herbaceous* ROIs, and only in the in-season comparison; while they may be statically significant the normalized differences are only 4 and 3 percent, respectively. These results for the combined parameters (**Δ**d, FP, and NDs)—ie. those calculated from more basic parameters—are similar to those found by both Kong *et al.* (2014) and Bourgeau-Chavez *et al.* (2013a), showing small normalized differences. In the current study, the *shrub and tree* ROIs showed no statistically significant differences in either comparison; again, this likely due to the nature of the *shrub and tree* grouping.

For the parameters showing the greatest normalized differences in the *herbaceous* ROIs (C-LL, C-LR, C-RR, C-VV, C-HH, vZ volume, vZ surface, vZ double, FD volume, FD surface, FD double, Pr_{max}, $Pr_{min,}$ S_{max} and S_{min}), 11 of the 16 showed greater differences in the extreme comparison than the in-season, averaging (median) approximately 4% higher. Of these C-HV, C-RR, C-LL, vZ volume, FD volume, and Pmin had the greatest differences, averaging 11% greater in the extreme comparison. In both the vZ and FD decompositions, the volume bounce show relatively large differences (16.5 and 9.8%, respectively) while their odd and double bounce results have slightly greater differences (~1-3%) in the in-season comparison. This suggests that volume bounce is affected to a greater extent by the seasonal vegetation difference of the extreme comparison than the odd and double bounce, making odd and double bounce more useful over a broader set of

vegetation conditions. A similar effect is noticed in the linear backscatters where C-HV has a 10% greater difference for the extreme comparison while C-HH and C-VV are 3.5 and -0.5, respectively, and in the circular backscattering where both C-LL and C-RR have greater extreme differences (~9%) compared to C-LR at ~2%. These results are all consistent with the expectation that by their nature vZ volume, FD volume, C-HV, C-LL, and C-RR tend to be more greatly affected by vegetation state. The intention of the in-season comparison was to negate these effects of differing seasonal vegetation state on the normalized differences, and as demonstrated, the above noted parameters do indeed show statistically significant normalized differences for the in-season comparison which can be attributed to different moisture conditions and not increased vegetation.

Conclusions

The current study builds on previous analyses into the ability of C-band polarimetric synthetic aperture radar to distinguish between wet and dry drought code conditions through the comparison of RADARSAT-2 imagery taken at an incidence angle of 38.2°. It examines eight regions of interest within a Canadian grassland ecosystem using three images selected from a time-series of forty-five images. In addition to the two images representing the extreme wet and extreme dry conditions (in May and October, respectively) of the time-series, a third image was examined which had a relatively low drought code (ie. high moisture) and was also in October thus having a similar vegetation state to the extreme dry condition; this in-season condition provided a comparison unaffected by differential seasonal vegetation states. Polarimetric parameters and decompositions were examined and normalized differences were determined between imagery from both the extreme wet and dry conditions, and the in-season wet and dry conditions.

The results show statistically significant differences between the test conditions for a number of these parameters particularly for the *herbaceous* ROIs. The three circular polarizations (C-LL, C-LR, C-RR) and the co-polarized linear backscatters (C-VV, and C-HH), and to a lesser extent C-HV, all provide strong statistically significant differences. All three Freeman-Durden and van Zyl decomposition parameters show strong differences in the *herbaceous* ROIs, especially double-bounce, and with odd- and double-bounce being least affected by changes in vegetation. The polarimetric

discriminators Pr_{max}, $S_{max,}$ S_{min} and to a slightly lesser extent Pr_{min} show consistently strong differences for the *herbaceous* ROIs. All of these C-band polarimetric parameters showed their statistically significant differences in the in-season comparison thus demonstrating their utility to distinguish between wet and dry soil conditions in *herbaceous* ROIs independent of the vegetation state.

Bibliography

Abbott, K.N., Leblon, B., Staples, G.C., Maclean, D.A. & Alexander, M.E. (2007) Fire danger monitoring using RADARSAT - 1 over northern boreal forests. *International Journal of Remote Sensing*, 28 (6), pp.1317–1338.

Axelrod, D.I. (1985) Rise of the grassland biome, central North America. *The Botanical Review*, 51 (2), pp.163–201.

Baghdadi, N., Cerdan, O., Zribi, M., Auzet, V., Darboux, F., Hajj, El, M. & Kheir, R.B. (2007) Operational performance of current synthetic aperture radar sensors in mapping soil surface characteristics in agricultural environments: application to hydrological and erosion modelling. *Hydrological Processes*, 22 (1), pp.9–20.

Bailey, A.W., McCartney, D. & Schellenberg, M.P. (2010) *Management of Canadian Prairie Rangeland*. 10144 ed. Agriculture and Agri-Food Canada.

Bourgeau-Chavez, L.L., Garwood, G., Riordan, K., Cella, B., Alden, S., Kwart, M. & Murphy, K. (2007) Improving the prediction of wildfire potential in boreal Alaska with satellite imaging radar. *Polar Record*, 43 (04), pp.321–330.

Bourgeau-Chavez, L.L., Kasischke, E.S. & Rutherford, M.D. (1999) Evaluation of ERS SAR data for prediction of fire danger in a Boreal region. *International Journal of Wildland Fire*, 9 (3), pp.183–194.

Bourgeau-Chavez, L.L., Kasischke, E.S., Riordan, K., Brunzell, S., Nolan, M., Hyer, E., Slawski, J., Medvecz, M., Walters, T. & Ames, S. (2007) Remote monitoring of

spatial and temporal surface soil moisture in fire disturbed boreal forest ecosystems with ERS SAR imagery. *International Journal of Remote Sensing*, 28 (10), pp.2133–2162.

Bourgeau-Chavez, L.L., Leblon, B. & Charbonneau, F. (2013a) Evaluation of polarimetric Radarsat-2 SAR data for development of soil moisture retrieval algorithms over a chronosequence of black spruce boreal forests. *Remote Sensing of Environment*, 132, pp.71–85.

Bourgeau-Chavez, L.L., Leblon, B., Charbonneau, F.J. & Buckley, J.R. (2013b) Assessment of polarimetric SAR data for discrimination between wet versusdry soil moisture conditions. *International Journal of Remote Sensing*, 34 (16), pp.5709–5730.

Bourgeau-Chavez, L.L., Riordan, K. & Garwood, G. (2008) Monitoring Fuel Moisture and Improving the Prediction of Wildfire Potential in Boreal Alaska with Satellite C-Band Imaging Radar. *Geoscience and Remote Sensing Symposium, 2008. IGARSS 2008. IEEE International*, 3, pp.864–866.

Buckley, J.R. (2004) Enhanced classification of prairie landscapes using simulated RADARSAT-2 imagery. *Canadian Journal of Remote Sensing*, 30 (3), pp.510–516.

Buckley, J.R. (2002) Environmental change detection in prairie landscapes with simulated Radarsat 2 imagery. *Geoscience and Remote Sensing Symposium, 2002. IGARSS '02. 2002 IEEE International*, 6, pp.3255–3257.

Buckley, J.R. (2008) Polarimetric Classification of Vegetation in Prairie Landscapes. *Geoscience and Remote Sensing Symposium, 2008. IGARSS 2008. IEEE International*, 3, pp.III–704–III–707.

Chen, Y. (2013) *Retrieving surface peat moisture in an Albertan bog with Radarsat-2,* MSc Thesis, University of Alberta

Cloude, S.R. & Pottier, E. (1997) An entropy based classification scheme for land applications of polarimetric SAR. *IEEE Transactions on Geoscience and Remote Sensing*, 35 (1), pp.68–78.

Cote, S., Muir, S., Srivastava, S.K. & Hawkins, R.K. (2009) SAR image quality and calibration operations for the RADARSAT satellites at the Canadian Space Agency. In: IEEE, pp.1–6.

Freeman, A. & Durden, S.L. (1998) A three-component scattering model for polarimetric SAR data. *IEEE Transactions on Geoscience and Remote Sensing*, 36 (3), pp.963–973.

Hajnsek, I., Jagdhuber, T., Schon, H. & Papathanassiou, K.P. (2009) Potential of Estimating Soil Moisture Under Vegetation Cover by Means of PolSAR. *IEEE Transactions on Geoscience and Remote Sensing*, 47 (2), pp.442–454.

Jarvis, A., Reuter, H.I., Nelson, A. & Guerara, E. (2008) SRTM 90m Digital Elevation Database v4.1 | CGIAR-CSI [Internet]. Available from: <http://www.cgiar-csi.org/data/srtm-90m-digital-elevation-database-v4-1> [Accessed 19 March 2013].

Kim, Y. & van Zyl, J.J. (2009) A Time-Series Approach to Estimate Soil Moisture Using Polarimetric Radar Data. *IEEE Transactions on Geoscience and Remote Sensing*, 47 (8), pp.2519–2527.

Kong, M.D., Leblon, B., Mathieu, R., Gross, P., Buckley, J.R., Naidoo, L. & Bourgeau-Chavez, L.L. (2014) Use of Radarsat-2 polarimetric SAR images for fuel moisture mapping in the Kruger National Park, South Africa. *Geoscience and Remote Sensing Symposium (IGARSS), 2014 IEEE International*, pp.5033–5036.

Lawson, B.D. & Armitage, O.B. (2008) *Weather Guide for the Canadian Forest Fire Danger Rating System*. Natural Resources Canada. Available from: <http://cfs.nrcan.gc.ca/publications/download-pdf/29152>.

Leblon, B. (2001) Forest wildfire hazard monitoring using remote sensing: A review. *Remote Sensing Reviews*, 20 (1), pp.1–43.

Leblon, B. (2005) Monitoring forest fire danger with remote sensing. *Natural Hazards*, 35 (3), pp.343–359.

Leblon, B. Bourgeau-Chavez, L., San-Miguel-Ayanz, J. 2014. Use of remote sensing in fire management, in "*Current International Perspectives on Wildland Fires, Mankind and the Environment"*, B. Leblon and M. Alexander (Eds), Nova Publisher, ISBN 978-1-63463-718-3, Chapter 2, 67-99.

Leblon, B., Kasischke, E.S., Alexander, M.E., Doyle, M. & Abbott, M. (2002) Fire danger monitoring using ERS-1 SAR images in the case of northern boreal forests.

Natural Hazards, 27 (3), pp.231–255.

Lee, J.-S., Wen, J.-H., Ainsworth, T.L., Chen, K.-S. & Chen, A.J. (2009) Improved Sigma Filter for Speckle Filtering of SAR Imagery. *IEEE Transactions on Geoscience and Remote Sensing*, 47 (1), pp.202–213.

Merzouki, A. & Leblon, B. (2011) Mapping fuel moisture codes using MODIS images and the Getis statistic over western Canada grasslands. *International Journal of Remote Sensing*, 32 (6), pp.1619–1634.

Oldak, A., Jackson, T.J., Starks, P. & Elliott, R. (2003) Mapping near-surface soil moisture on regional scale using ERS-2 SAR data. *International Journal of Remote Sensing*, 24 (22), pp.4579–4598.

Pasolli, L., Notarnicola, C., Bruzzone, L., Bertoldi, G., Chiesa, Della, S., Niedrist, G., Tappeiner, U. & Zebisch, M. (2011) Polarimetric RADARSAT-2 imagery for soil moisture retrieval in alpine areas. *Canadian Journal of Remote Sensing*, 37 (5), pp.535–547.

Rannie, W.F. (2001) The 'Grass Fire Era'on the southeastern Canadian Prairies. In: D. C. Munski ed. *Prairie Perspectives: Geographical Essays*. University of North Dakota, p.19.

Rowland, J.M. (2003) A New Approach to Selecting Sustainable Ecosystem Indicators: a Neural Network. Royal Military College of Canada. Available from: <http://www.collectionscanada.gc.ca/obj/s4/f2/dsk4/etd/NQ82841.PDF>.

Sokol, J., NcNairn, H. & Pultz, T.J. (2004) Case studies demonstrating the hydrological applications of C-band multipolarized and polarimetric SAR. *Canadian Journal of Remote Sensing*, 30 (3), pp.470–483.

Stiles, J.M., Sarabandi, K. & Ulaby, F.T. (2000) Electromagnetic scattering from grassland. II. Measurement and modeling results. *IEEE Transactions on Geoscience and Remote Sensing*, 38 (1), pp.349–356.

Stocks, B.J., Lawson, B.D., Alexander, M.E., Van Wagner, C.E., McAlpine, R.S., Lynham, T.J. & Dube, D.E. (1989) The Canadian Forest Fire Danger Rating System: An overview. *Forestry Chronicle*, 65 (6), pp.450–457.

Thoma, D.P., Moran, M.S., Bryant, R., Rahman, M., Holifield-Collins, C.D., Skirvin, S., Sano, E.E. & Slocum, K. (2006) Comparison of four models to determine surface soil moisture from C-band radar imagery in a sparsely vegetated semiarid landscape. *Water Resources Research*, 42 (W01418), pp.1–12.

Touzi, R. (2007) Target Scattering Decomposition in Terms of Roll-Invariant Target Parameters. *IEEE Transactions on Geoscience and Remote Sensing*, 45 (1), pp.73–84.

Touzi, R., Goze, S., Le Toan, T., Lopes, A. & Mougin, E. (1992) Polarimetric discriminators for SAR images. *IEEE Transactions on Geoscience and Remote Sensing*, 30 (5), pp.973–980.

Trudel, M., Charbonneau, F.J. & Leconte, R. (2012) Using RADARSAT-2 polarimetric

and ENVISAT-ASAR dual-polarization data for estimating soil moisture over agricultural fields. *Canadian Journal of Remote Sensing*, 38 (4), pp.1–14.

Ulaby, F.T., Moore, R.K. & Fung, A.K. (1982) *Microwave Remote Sensing Active and Passive, Volume II Radar Remote Sensing and Surface Scattering and Emission Theory*. Norwood, Artech House Inc.

Van der Sanden, J.J. (2004) Anticipated applications potential of RADARSAT-2 data. *Canadian Journal of Remote Sensing*, 30 (3), pp.369–379.

Van Wagner, C.E. (1987) *Development and Structure of the Canadian Forest Fire Weather Index System*. Ottawa, Canadian Forestry Service. Available from: <http://cfs.nrcan.gc.ca/pubwarehouse/pdfs/19927.pdf>.

Van Wagner, C.E. & Pickett, T.L. (1985) *Equations and FORTRAN Program for the Canadian Forest Fire Weather Index System*. Ottawa, Canadian Forestry Service. Available from: <http://cfs.nrcan.gc.ca/pubwarehouse/pdfs/19973.pdf >.

van Zyl, J.J. (1989) Unsupervised classification of scattering behavior using radar polarimetry data. *IEEE Transactions on Geoscience and Remote Sensing*, 27 (1), pp.36–45.

van Zyl, J.J. & Kim, Y. (2011) *Synthetic Aperture Radar Polarimetry*. Hoboken, New Jersey, John Wiley & Sons, Inc.

van Zyl, J.J., Arii, M. & Kim, Y. (2011) Model-Based Decomposition of Polarimetric SAR Covariance Matrices Constrained for Nonnegative Eigenvalues. *IEEE*

Transactions on Geoscience and Remote Sensing, 49 (9), pp.3452–3459.

van Zyl, J.J., Zebker, H.A. & Elachi, C. (1987) Imaging radar polarization signatures: Theory and observation. *Radio Science*, 22 (4), p.529.

Wagner, W. & Scipal, K. (2000) Large-scale soil moisture mapping in western Africa using the ERS scatterometer. *IEEE Transactions on Geoscience and Remote Sensing*, 38 (4), pp.1777–1782.

Wagner, W., Noll, J., Borgeaud, M. & Rott, H. (1999) Monitoring soil moisture over the Canadian Prairies with the ERS scatterometer. *IEEE Transactions on Geoscience and Remote Sensing*, 37 (1), pp.206–216.

Wang, Y., Kasischke, E.S., Bourgeau-Chavez, L.L., O'Neill, K.P. & French, N.H.F. (2000) Assessing the influence of vegetation cover on soil-moisture signatures in fire-disturbed boreal forests in interior Alaska: Modelled results. *International Journal of Remote Sensing*, 21 (4), pp.689–708.

CURRICULUM VITAE

Duncan Dawson Rand, P.Eng

University of Salford, Postgraduate Diploma in Geographical Information Systems with Distinction, 2012

University of Alberta, Bachelor of Science in Civil Engineering, 1992